geosciences

MDPI

Article

A Kinetic Explanation for Combined Potassium Gains and Radiogenic ^{40}Argon Losses of Diagenetic Illite-Rich Clay Separates

Norbert Clauer [1,*] and Abraham Lerman [2]

[1] Institut des Sciences de la Terre et de l'Environnement, Université de Strasbourg (UdS/CNRS), F-67084 Strasbourg, France
[2] Department of Earth and Planetary Sciences, Northwestern University, Evanston, IL 60208, USA; alerman@northwestern.edu
* Correspondence: nclauer@unistra.fr

Abstract: In this study, a kinetic model sketches the concomitant K gain and radiogenic ^{40}Ar loss of clay separates recovered from progressively buried sediments. Published K-Ar ages of clay separates from the Mahakam Delta, the Texas Gulf Coast, and the North Sea were used to constrain the modeling. As compared with analytical results, the model simulates changes relative to depth or to deposition time of the K-Ar ages from fine- and coarse-grained clay crystals. The decrease in the K-Ar ages of detrital-rich coarse-grained fractions (>2 µm) is bracketed with depth by K addition rates between 0.2 and 3.5%/Ma and slightly higher ^{40}Ar release rates between 0.5 and 4.5%/Ma. The former rate varies from 3.5 to 6%/Ma in the fine-grained fractions (<0.4 µm) and the latter rate varies from 0.7 to 6%/Ma in the same fractions. In fact, the K addition and the radiogenic ^{40}Ar release rates record independent processes on different material sizes and types. Small K addition and ^{40}Ar escape rates of about 1%/Ma also simulate analytical cases in which the mean K-Ar ages of the finer grained fractions remain about constant with increasing depth, confirming that the relationship between K-Ar age and stratigraphic depth cannot represent a temporary "steady state", but a continuing dynamic process at a smaller rate. In turn, the modeled results help quantifying the illitization reactions in size separates consisting of authigenic and detrital clay materials from sediments covering stratigraphic intervals from 10 to 1000 Ma.

Keywords: burial diagenesis; illitization; K gain; radiogenic ^{40}Ar loss; K-Ar ages; K-Ar two process model; sediment sequences; basin sedimentary evolution

Citation: Clauer, N.; Lerman, A. A Kinetic Explanation for Combined Potassium Gains and Radiogenic ^{40}Argon Losses of Diagenetic Illite-Rich Clay Separates. *Geosciences* **2022**, *12*, 186. https://doi.org/10.3390/geosciences12050186

Academic Editors: Jaime Cuevas Rodríguez and Jesus Martinez-Frias

Received: 21 March 2022
Accepted: 11 April 2022
Published: 25 April 2022

1. Introduction

For a long time, the post-depositional evolution of clay minerals has been considered to be determining information for delineating the diagenetic evolution of sedimentary sequences at different time scales and in varied application fields. Hydrological characterization of oil- and gas-bearing reservoirs and of deeply buried waste-hosting repositories, fluid–rock interactions and mass transfers by fluid migrations in the subsurface, as well as gas exchanges with the atmosphere are some of the potential applications. Moreover, burial-induced diagenetic changes in sediments have often been characterized and quantified by the well-known conversion change from smectite to illite/smectite mixed layers (labeled I-S hereafter) and ultimately to illite, the trend being visualized by a progressive increase in K (e.g., [1–3]). This systematic increase of K in I-S with burial depth explains, at least partly, the decrease in the K-Ar isotopic ages of progressively buried clay-rich size fractions dated in such contexts (e.g., discussion in [4]). Radiogenic ^{40}Ar, as well as radiogenic ^{87}Sr in the case of the Rb-Sr method with similar "age" reductions, are theoretically only incorporated into newly crystallized illite-type structures when ^{40}K and ^{87}Rb start to decay. The addition of in situ crystallized illite crystals with high K contents and no radiogenic ^{40}Ar at the

time of their crystallization means that the K and Ar contents of size fractions consisting of detrital and newly formed crystal mixtures yield more K and less radiogenic ^{40}Ar, as is the case for the radiogenic ^{87}Sr in the Rb-Sr method. Furthermore, radiogenic ^{40}Ar has also been assumed, on the basis of various theoretical models, to diffuse preferentially out of the smallest clay-type crystals, as the other Ar isotopes, because of the particle size. This theoretical diffusion has never been demonstrated analytically, only suggested by mathematical models (e.g., [5]) by authors who completed a molecular modeling of the behavior of the ^{40}K during its natural radioactive decay into ^{40}Ar. They concluded that, due to high kinetic energy, some of the decayed ^{40}Ar atoms may potentially leave the interlayer position to embed nearby or into the opposite tetrahedral sheet of the next silicate layer. The age decrease should even be higher for thinner crystals, but this has never ibeen demonstrated on a straight analytical basis. Also, any radioactive K located at the edges of crystals or elsewhere that decays into radiogenic ^{40}Ar should clearly be identical to any other radioactive element that has been used, for decades, for isotopic dating. However, if such escape is facilitated by the fact that Ar is a neutral atom, the assumption may become questionable. The amount of radiogenic ^{40}Ar at the edges of illite crystals can reasonably be considered to be quite limited, the loss would be, most probably, within the analytical uncertainty of the method, as radioactive K represents no more than 0.012% of the total K present in illite-type crystals, even of nanometer size. It is also worthwhile noting that the analytical data currently available systematically show that nanometer-sized illite-rich bentonite separates devoid of any detrital addition are sometimes older, and not younger as suggested by the model, than strictly contemporaneous crystals (e.g., [6]). Alternatively, those with younger ages could also have been subjected to radiogenic ^{40}Ar release relative to the older counterparts, which has another drawback; the younger age values being the most common and not the exceptions. Furthermore, nanometer-sized clay crystals are the smallest crystals that can be isolated presently, and those separated from detrital-free bentonite layers do not indicate any radiogenic ^{40}Ar diffusion [6]. Isolated nanometer-sized crystals are far larger than the critical size for mechanical Ar diffusion at the angstrom-sized interlayer edges, suggesting in turn that the size of the crystals is not of a concern. Indeed, the size of the crystal is still not a determining argument for the escape of radiogenic ^{40}Ar as argued for a long time (e.g., discussion in [4]). So far, there is no solid analytical argument to support any physical spontaneous extraction of atmospheric or radiogenic Ar from clay crystals, which are both squeezed exactly the same way in the same interlayer sites, not locked, only hold by a Van der Waals force, as is the case for any neutral atom and molecule.

The present modeling attempt consists of a mathematical quantification of the K gain rates and the radiogenic ^{40}Ar loss rates of size fractions that consist of mixed authigenic and detrital I-S. The diagenetic transformation of smectite into illite along an I-S trend is considered to reflect the changing ^{40}Ar/^{40}K atomic ratio, and consequently the K-Ar age values of the size fractions. In addition to the ^{40}Ar/^{40}K ratio, the K-Ar "apparent ages", in the sense of not having necessarily a geological meaning, represent progressive changes in the smectite-to-illite transition. Induced by a temperature increase and, therefore, by increasing depth of the host sediments, the application of clay-type size fractions to their K-Ar apparent ages is not straightforward even if simple. The recurrent reason is the almost systematic and variable occurrence of detrital particles that depend on the pre-depositional history of the host sediments, which are consequently of variable mineral composition and crystallographic status. Detrital illite/muscovite material occurs quite systematically in the isotopic dating of any authigenic K-rich illite particle, even by separating size fractions into a nanometer range, as already studied and discussed (e.g., [7]).

2. The Handling of Detrital and Authigenic Illite Mixtures

Very importantly, Ar of any origin, i.e., radiogenic or atmospheric, is expelled from clay crystals of any size only when the surrounding thermal-chemical conditions impact the integrity of the host crystals in order to facilitate expulsion, in the case of a supply or a release of K. A changing impact is most often induced by an increase in temperature as

compared with a change induced by the chemical environment, for instance by migrating fluids. Whatever the process, it will not induce Ar release from authigenic crystals, as these take advantage of a more favorable environment than dissolving or simply altering. In fact, a changing thermo-chemical environment affects detrital crystals. Since authigenic crystals do not, at the time, contain radiogenic ^{40}Ar, burial does not explain the reduction of its content. In contrast, detrital crystals that are affected by the same thermal-chemical environment as compared with the authigenic crystals, are progressively altered, and consequently, progressively loose radiogenic ^{40}Ar, and possibly some K by a smectitization of the illite structure. This suggests that this combined process is an appropriate mechanism by which radiogenic ^{40}Ar and also K can be released from illite-type crystals of various sizes, which does not depend on the amounts of detrital and authigenic illite crystals or on the size of the crystals. An efficient check of this hypothesis can also be provided, for example, by the analysis of authigenic mineral populations separated from detrital populations by size fractionation.

Isotopic dating of diagenetic illite in sedimentary rocks remains to be an overall repetitive challenging task in each new study based on any isotopic method, because of the permanent need to successfully separate the authigenic from the intimately mixed detrital components. In fact, beyond the fact that authigenic crystals are often smaller than their associated detrital counterparts, the systematic difficulty associated with separating both can be due, but not only, to sample preparation. In recent years, preparation aspects have been discussed to evaluate how the results may depend on the separation and preparation used by the investigators (e.g., [8]). Their review, complemented by an evaluation of the benefits of size fractionation to obtain meaningful stratigraphic ages of clay minerals [9], was not intended to grade sample preparations or investigators' duties. The aim was simply to discard inappropriate preparation procedures and to suggest replacement techniques for a very specific method to separate authigenic and detrital clay-rich materials. Notably, sometimes it is impossible to separate authigenic and detrital illite-rich clay crystals using the presently available methods (e.g., [7]), and therefore, there is a need to evaluate compensatory tools for extrapolating the crystallization age(s) of authigenic illite from any mixture that does not yield reliable stratigraphic age records. A way to overcome the difficulty is to treat a database by using a mathematical simulation of the content of each K-bearing mineral type in different separates in order to extract the theoretical age of the authigenic component from the overall available K-Ar database.

Elliott et al. [10] and Mossmann [11] were the first to report on such modeling, while others essentially based their attempts on the timing of the smectite into illite transformation [12–15]. The attempt by Lerman et al. [16] was different as it focused on the sole behavior of the K and the radiogenic ^{40}Ar of mixed detrital and authigenic clay separates that either altered or crystallized during a progressive burial-induced temperature increase. Szczerba and Środoń [17] published another model based on the K-Ar reciprocal evolution by elaborating again on the extraction of meaningful "ages" of the authigenic component of mixtures on the basis of mineralogical criteria, but they did not discuss how burial-induced diagenesis could affect the K-Ar system of the mixtures. In summary, the physical-chemical repercussions of a diagenetic impact on I-S are the variable gain rates of K and the variable loss rates of radiogenic ^{40}Ar from variably sized separates depending on their relative contents of authigenic and detrital materials. These changes depend on the burial depth, that is to say, the related temperature increase, which means that there is a need to evaluate separately the changing rates of the K gain and of the radiogenic ^{40}Ar loss. The parameters evolve concomitantly, but it is not clear if their impacts are identical on the K-Ar system of detrital and authigenic clay components relative to a temperature increase.

Over the years, the K concentration increase in I-S with increasing illite content has been reported when burial of the host sediments increases (e.g., [18–24]), although a loss of SiO_2 during the smectite-to-illite trend can also induce a relative K enrichment. It has also been evidenced, over the years, that radiogenic ^{40}Ar forming ubiquitously from ^{40}K is released from clay lattices at an increased rate when the particle size decreases,

providing, in turn, lower K-Ar age values for finer grained fractions when combined with the abovementioned addition of K (e.g., [4] and references therein, [9,25–27]), although the age difference may also correspond to a higher content in authigenic material relative to its detrital counterpart. The $^{40}Ar/^{40}K$ ratios and the related K-Ar age values of clay separates of any size consisting of mixtures of authigenic and detrital particles do, then, reflect two processes: (1) an addition of K but no immediate addition of radiogenic ^{40}Ar during the crystallization of new nuclei on or next to older detrital grains, and (2) a loss of radiogenic ^{40}Ar from progressively altered detrital crystals. These processes can operate simultaneously, but independently and variably, depending on the size of the particles and on the evolution state of both the detrital and authigenic minerals, but not on their relative amounts.

Although models that independently interpret a K addition into or a ^{40}Ar release from clay-sized particles have already been published, it is important to reiterate that the approach here is based on an independent two-type mechanism that integrates an addition and a loss of two different isotopes. The approach in this study is also compared to, and therefore, constrained by independently available K-Ar data of four sections of shales and sandstones for which varied clay-type separates have already been measured and published. In summary, this approach was tested with real isotopic analyses of buried illite-rich size fractions consisting of mixtures of different stratigraphic ages in various depositional basins. The belief is that this comparison with analytical data is a direct control of the calculations and, therefore, gives supplementary strength to the numerical attempt.

3. A Model for a Combined K Gain and Radiogenic ^{40}Ar Loss

The present exercise integrates a K gain and a ^{40}Ar diffusion that happen simultaneously in clay crystals during a progressive burial with independent rates and parameters that constrain and explain the simultaneous gain and loss. The goal here was the use of changing K-Ar apparent ages of clay mixtures relative to burial that improve the sorting out of physical-chemical processes of various grain sizes at increasing temperatures. The challenge was not at all the explanation of potential "ages" of mixed authigenic and detrital components, or of pure restored end members, which has already been addressed. The two identified processes become necessarily dominant for the K-Ar system of clay fractions at increasing depth, as they occur concomitantly but remain independent at the data level. Indeed, the K gain does most probably not affect the detrital mass of the separates and, similarly, the ^{40}Ar loss certainly does not affect the authigenic fraction of sized separates for the reasons already discussed in the previous sections.

A diffusion/gain attempt, similar to that evaluated here, needs to address some constraints, although not the origin of the source material, for which no analytical consensus seems to exist anyway (e.g., [20,28–32]). In fact, the origin of the detrital materials, either sedimentary, metamorphic, or plutonic, does not impact their K-Ar ages. Conversely, for example in the Rb-Sr method, the origin of the detrital material can have an impact on the initial $^{87}Sr/^{86}Sr$ ratio of the detrital population, while that of the authigenic materials strictly depends on the depositional or diagenetic environment. Another aspect not well constrained that needs to be included in the attempt is how illitization proceeds, either continuously or episodically by a nearby or far tectonic-thermal impact of anchi- to epi-metamorphic instantaneous or lasting events. Even if it is widely admitted that burial-driven illitization is a continuous process, often without analytical data but with the agreement that most of the smectite-to-illite changes occur within a limited thickness in the upper section of the sediments, until the upper temperature limit of illite precipitation. Since Kübler [33], many have reported various burial-induced diagenetic evolutions that highlighted a decrease in the I-S expandability relative to depth, and therefore, to a temperature increase by either continuous burial or episodic tectonic events.

The present kinetic exercise is based on changes in the $^{40}Ar/^{40}K$ ratios and, therefore, of the K-Ar ages from finer- (<0.4 or <0.1 μm) and coarser-grained (generally >2 μm) fractions relative to the burial evolution of three independent sedimentary sequences. These

sequences belong to the Late Oligocene-Early Miocene section (34 to 20 Ma) of the Texas Gulf Coast [25,34], the Mesozoic sequence (Early Jurassic to Late Cretaceous, from 190 to 78 Ma) of the North Sea in the Bergen high area [22] and the Neogene (1 to 20 Ma) shales and sandstones of Eastern Borneo [24,35]. These sequences were selected because they compile enough K-Ar data on various size fractions that are scattered widely over their stratigraphic intervals and are significantly older than the deposition time. Again, the present attempt was thought to show that the decrease in the K-Ar ages of clay fractions consisting of detrital and authigenic components, can be framed by kinetic rates combining a release of radiogenic ^{40}Ar with an addition of K to clay crystals, when depth and temperature increase, with similar crystallographic characteristics but of different origins. The model was also thought to provide a realistic interpretation of the K-Ar system from illite-type materials with analytically constant K-Ar data of fine-grained shale fractions that range over variable depth ranges [4,22,36]. Such constant K-Ar age data are somehow unexpected after the above description unless the independent rates of K gain and ^{40}Ar loss are close enough to simulate constant age values. This situation of constant age values is admittedly difficult to consider for two independent processes that occur in the same mineral type of similar grain size, different origins and evolutions, positive and negative. Although they have been explained as "steady state" during an extended period of time (given by the depth), or were viewed as "punctuated" [37], such constant K-Ar evolution steps have no reality at short time scales, as already discussed [38], unless magnified by punctual tectonic-thermal events.

4. Review of the Analytical Database

The numerical base used for the modeling attempt yields, on purpose, very distinct aspects that are of importance for the validity of the simulation, such as different stratigraphic ages, various types of extracted clays and specific evolutions in various depositional basins. These differences are somehow important as they make the evaluation of the results more accurate and the calculation more general. Among the three selected basins, the Gulf Coast is a broadly subsiding continental margin that received and still receives smectite-type materials of pedogenic and crustal origin from the continental interior of North America. The Bergen High in the North Sea is characterized by significant basement adjustments that induced block faulting, tectonic-induced fluid migrations and a Caledonian detrital supply into a narrow marine area between Scandinavia, Greenland and North America [39]. The Mahakam Basin of Eastern Borneo is still subsiding in a tectonically active region that receives Late Cretaceous to present-day detritus.

In the three sedimentary sequences for which the clay fraction was already analyzed, the amount of illite layer from I-S changed quite similarly relative to depth. The illite-type material increased downwards in the three selected sedimentary sequences, from 15 to 80% in the Gulf Coast, from 60 to 95% in the North Sea section, and from 10 to 80% in the Mahakam shales and sandstones. These trends mimic the concentrations of K (in wt.%) and ^{40}Ar (in 10^{-10} mol/g) in the rock sections of the three basins (Figure 1). In the Mahakam section, as is probably also the case in the other basins, the analyzed K and the radiogenic ^{40}Ar contents of the <0.4 µm fraction reflect variable contents of K-free diluting minerals, such as kaolinite and chlorite together with probable carbonates, sulfates, and chlorides that show various relative amounts of authigenic and detrital clay-type particles. Although the three sedimentation basins had different histories, various origins and scattered K-Ar ages for the detrital clay materials, diverse depositional ages for the sediments, and variable depths at which the sediments were buried, the K-Ar system of the fine-grained size fractions from shales showed noticeable similarities at different depths [40]. These similarities suggest that the K-Ar system of the fine-grained fractions recorded a coherent evolution of the constitutive illite-rich material that was clearly disconnected from parameters such as rock lithology, tectonic evolution, or temperature gradient. The K content of the K-hosting minerals (K_{adj}) was consistently increasing with depth, in agreement with a diagenetic illitization (Figure 1). However, the fact that the

sources of K were not well constrained suggests a continuous supply with changing rates. Changes in the initial ^{40}Ar and ^{40}K contents of the particles at the time of deposition were not considered here, as well as various diagenetic rates and mechanisms that most likely account also for the scatter of the data. In addition, strong analytical constraints would not better constrain the concept of the model.

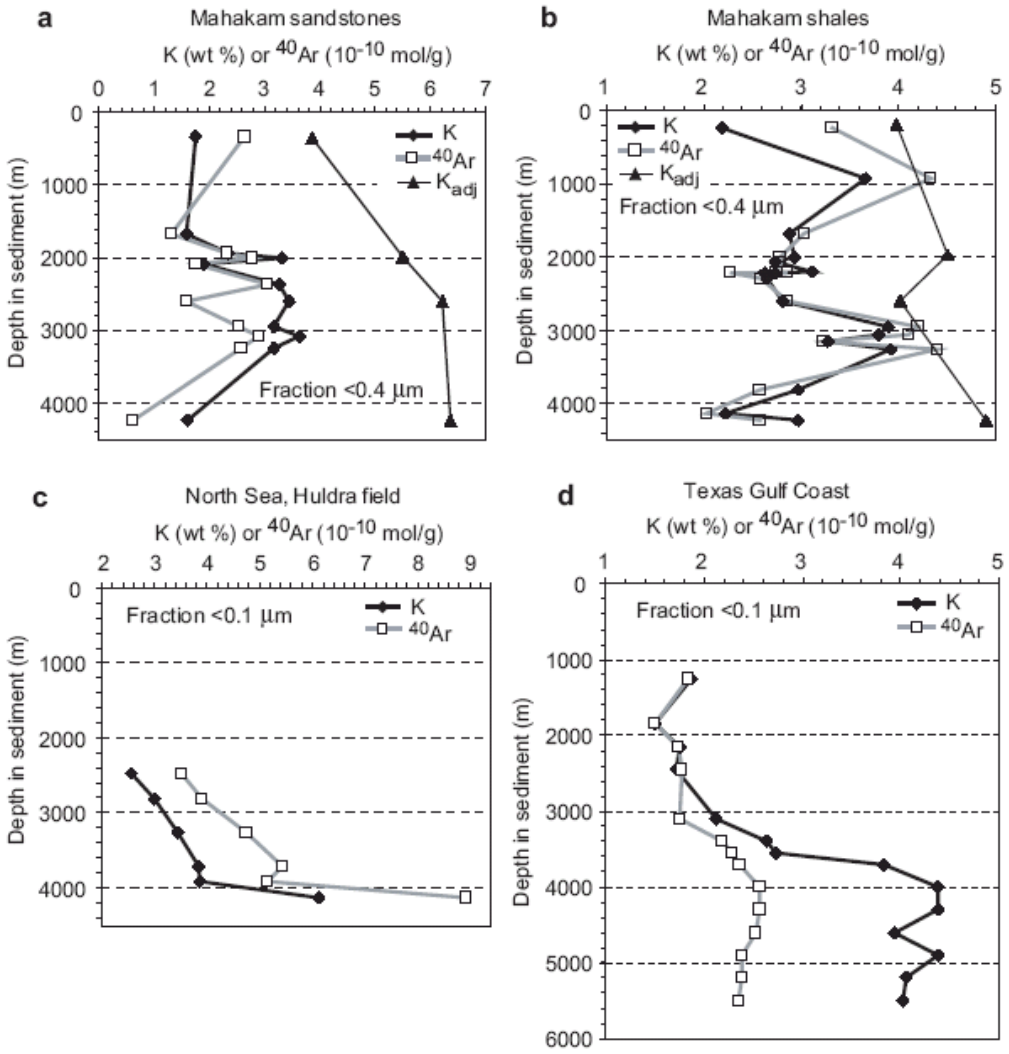

Figure 1. Potassium (K in wt.%) and radiogenic ^{40}Ar (10^{-10} in mol/g) contents of the fine-grained clay fractions in: (**a**) the sandstone of the Mahakam Delta Basin; (**b**) shale sections of the Mahakam Delta Basin [36]; (**c**) the section in the North Sea, Bergen High area [22]; (**d**) the section in the Texas Gulf Coast [37]. In (**a**,**b**), K is the concentration in the whole <0.4 µm fraction, K_{adj} is the concentration only in the K-bearing mineral phases illite and I-S of the same <0.4 µm fraction [24]. Note the differences in the horizontal scale of the figures.

The K-Ar ages of the illite-rich clay separates from the three sequences are reported on the basis of the K content and the calculated ^{40}K and radiogenic ^{40}Ar concentrations (Figure 2). The lack of analytical uncertainties at successive steps of the modeling is also clearly assumed, as mentioned above, due to the fact that it would be premature, because of the limited database so far available, to take into consideration the analytical uncertainties in the calculations. However, it should be noted that the mean uncertainty of the analytical K-Ar ages, here, ranged from ±2 to ±4% of the reported values and that this uncertainty was taken into consideration in the calculations. The ^{40}Ar/^{40}K ratios and the corresponding K-Ar apparent ages decrease downwards into the 1700 to 4000 m thick sediment sections, which corresponds to depositional age intervals of about 14 Ma in the Gulf Coast, 20 Ma in

the Eastern Borneo, and 110 Ma in the North Sea. The K-Ar ages of the clay materials from the Mahakam Delta and the Gulf Coast sections (Figure 2a,b,d) are older than the stratigraphic/depositional age, implying material sources with an overload of detrital crystals, various evolution rates for the detrital material, and changing authigenic/detrital ratios for the mixtures. Of special interest is the fact that the fine-grained fractions yield about constant K-Ar apparent ages over extensive depth intervals in the three shale sequences: between 2000 and 4000 m in the Mahakam Delta Basin, between 2500 and 4000 m in the North Sea site, and twice in the Gulf Coast sequence between 1200 and 2400 m and between 3600 and 5500 m. Although the similarity of such K-Ar trends in themselves does not explain why the K-Ar system behaves like that, the model tested here is considering these trends by combining K gain and ^{40}Ar loss at specific rates so that the obtained K-Ar age data do also appear constant. This interpretation is certainly a reasonable alternative to the suggested steady state or a punctuation behavior during a given period of time or interval of depth that has no scientific ground.

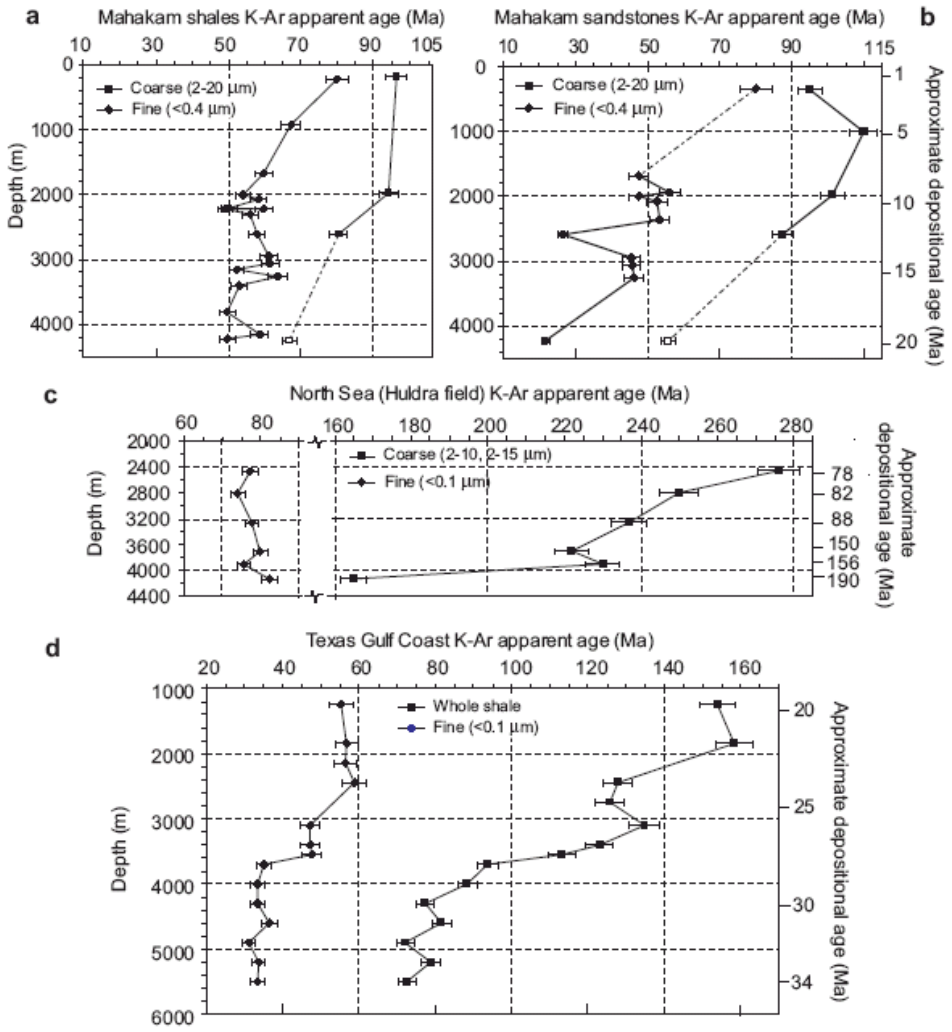

Figure 2. K-Ar apparent ages of the coarse- and fine-grained size fractions from: (**a**) the shales of the Mahakam Basin; (**b**) the sandstones of the Mahakam Basin [24,36]; (**c**) the sequence of the Huldra field in the North Sea [22]; (**d**) the sequence of the Gulf Coast [37]. The K-Ar ages in the latter were recalculated using the atomic ratio $^{40}K/K = 1.167 \times 10^{-4}$, $\lambda = 5.543 \times 10^{-10}$ yr^{-1}, and $\lambda_a = 5.810 \times 10^{-11}$ yr^{-1} [41]. Two of the lines are partly dotted when the two successive samples are quite distant.

In summary, the K-Ar ages of various clay size fractions, even if not numerous presently, appear to be consistent and coherent in sediments that are different in their deposition times, in the provenance of their detritus, and in the depositional and structural context of the basins. In fact, such variable situations are solid arguments for a modeling attempt, even considering that some of the calculated parameters are not as constrained as they should be, because the process seems to follow rules that are applicable to any first-order basin, independently from local aspects. At last, but not least, the alteration process of the K-carrier detrital materials that are mostly mica and K feldspar in the coarse-grained fractions varies along a sedimentation column as it does in different size fractions, which has not yet been extensively studied. In fact, only a few results of very coarse-grained fractions (40–63 μm) of buried sediments from the Mahakam shales [40] show a K-Ar system altered only below 2000 m depth at a temperature significantly higher than that inducing either authigenic illite crystallization and/or detrital illite/mica alteration. This example confirms that illite authigenesis proceeds mainly in the upper parts of basins, whereas alteration and dissolution of micaceous detrital particles occur in deeper parts of basins. When combined, the two processes display a dominant gain of K in the upper depositional sections and a dominant loss of radiogenic ^{40}Ar in the deeper sections. However, as a first step, the process has been restricted to a continuous addition of K and loss of radiogenic ^{40}Ar over various time intervals, as can be extracted from analytical data, even if this appears to oversimplify the mathematical approach. In fact, the goal, here, was not a new interpretation of the data, but a gathering of new information based on simultaneous, but independent K gain and ^{40}Ar loss rates, in order to identify which of these two parameters is predominantly monitoring the rates and especially when, and also to explain "steady" results at a depth, for which scientifically sound interpretations are still lacking, at least to us.

5. Modeled ^{40}Ar Losses and/or K Gains in K-Ar Apparent Ages of Clay Materials

Minerals deposited in a basin can be considered to be systematically of various provenances based on the variable ^{40}Ar/^{40}K ratios of those carrying K, which depends, in turn, on the extent of mixing of variably sized single crystals or crystal agglomerates. However, the source of detrital minerals, especially of clay type, is probably less important for their K-Ar system than the interactions they underwent during continental weathering, erosion, and riverine transport before final deposition. In fact, scattered K-Ar ages of clay materials from upper sedimentary sequences are often framed by a physical homogenization during the river transport and marine mixing. In contrast, if detrital clay crystals would have remained unaltered since continental erosion and weathering until burial, subsequently behaving as closed K-Ar systems, their ^{40}Ar contents would have continuously increased due to the sole decay of ^{40}K, as would have their K-Ar ages relative to time or depth in the sediment. In fact, this is never the case as detrital minerals, and especially their K-Ar systems, do not function as closed systems [42], at least the very small nanometer-sized minerals.

A general model for clay minerals in which addition of K and loss of ^{40}Ar operate simultaneously is given by the Equation (1):

$$\underset{\text{K addition}}{d(^{40}\text{Ar})/dt} = \underset{^{40}\text{Ar growth}}{\lambda_a {}^{40}\text{K}_0(1+bt)e^{-\lambda t}} - \underset{^{40}\text{Ar escape}}{\varepsilon(^{40}\text{Ar})}, \quad (1)$$

where ^{40}Ar and ^{40}K are the nuclide concentrations in the clay mixture in mol/g, and the values of the decay-rate constants λ_a and λ are provided in the Appendix A (available upon request). Here, the ^{40}K is incorporated by the particles at a linear rate b in units of Ma^{-1}, although other modes of K gain or loss are conceivable. Moreover, the ^{40}Ar produced by the decay of ^{40}K was portrayed as escaping from altering illite particles at an ε Ma^{-1} rate, making such a behavior a first-order flux dependent on the ^{40}Ar concentration in the crystals. To simplify the mathematical procedure, the parameter rates b and ε were chosen to be constant, although they vary naturally during deposition in different basins. In fact, changing the rates based on specific parameters that are not of first order would

render the model to have little practical value. Simplified versions of the two-process model include a case of ^{40}Ar loss from crystals without K addition ($\varepsilon > 0$ and $b = 0$, [28]) and a case of K addition at either a linear ($\varepsilon = 0$ and $b > 0$) or an exponential (e^{bt}) rate. Potassium loss, although much less documented analytically than its gain by clays, is also taken into consideration in Equation (1) by a negative value for the rate parameter b ($b < 0$); solutions of the calculations are provided in the Appendix A. No ^{40}Ar escape combined with a K addition and $\varepsilon = 0$ and $b = 0$ in Equation (1) describe the theoretical closed system (given in the Part 1 of the Appendix A). This unrealistic case is only provided as a mathematical reference, knowing from analyses that radiogenic ^{40}Ar is stored by the K-rich component of any illite-type mixture, but the same mixture can also lose radiogenic ^{40}Ar and K when the crystals are detrital and are subjected to progressive alteration. The addition of K to I-S crystals into the illite layers during burial diagenesis induces, necessarily, a decrease in the K-Ar apparent ages, the linear rate of K addition in Equation (1) describing the growth of the authigenic mineral mass, which is different from the growth of a characteristic linear dimension.

As K addition, ^{40}Ar release from illite-type crystals induces a decrease of their K-Ar apparent ages. Numerous studies of K-containing silicate minerals, in laboratory and natural conditions of increasing temperature, have reported such ^{40}Ar escapes (e.g., [43–45]). Therefore, it cannot be completely excluded that excess ^{40}Ar may also occur at a small scale in newly formed particles depending on their immediate environment, especially if affected by an alteration process. For instance, the search of excess ^{40}Ar in the pore system of natural shales was documented by a simple experiment (Clauer, unpublished data) based on the extraction of gas from the pores of rock chips from three samples maintained under vacuum during a week at a temperature of about 40 °C, and by measuring afterwards the ^{40}Ar/^{36}Ar of the collected gas. The gas ^{40}Ar/^{36}Ar ratio averaged 315 ± 5 (2σ), which was slightly but significantly above the 298.6 ± 0.4 (2σ) for the atmospheric ratio [46], while the control of the atmospheric ^{40}Ar/^{36}Ar ratio was 296.0 ± 0.5 (2σ) for the mass spectrometry at the time of the experiment. This unique result of a simple not-well constrained experiment does not represent the general rule. However, it suggests that a measurable ^{40}Ar overpressure may exist in the pore system of shales, probably because of alterations in the detrital K-carrier minerals, and that this environmental Ar could be incorporated by the authigenic illite crystallizing in the shale pores with such Ar "overpressure". For completeness, it cannot be denied that the result of this simple experiment may also support, indirectly, some of the conclusions of Szczerba et al. [5]. Indeed, these authors concluded that due to their high kinetic energy, ^{40}Ar atoms can potentially be removed from interlayer positions of authigenic illite crystals into their surrounding interlayers. Such atoms are, then, expected to leave the mineral particles over a long geological time, especially when located at crystal edges and can, potentially, end in the pore system of the host rocks. In any case, such a behavior can only be considered to be a limited side effect on K-Ar apparent ages of authigenic K-bearing crystals because of the very low amount of released radiogenic ^{40}Ar. Such release may also occur due to sample preparation and size fractionation, which both favor releases of any type of gas from solid samples. The limited amount of ^{40}Ar theoretically released by nucleating clay particles in the pore system of shales represents one of the parameters that are difficult to constrain and are also of a limited impact for the construction of a mathematical model. They will, therefore, be discarded hereafter.

As a preliminary test of the two-process model, K-Ar apparent ages were calculated for a theoretical clay mixture consisting of detrital particles with a K-Ar age of 55 Ma and authigenic crystals with an initial K-Ar age of 0 Ma that was buried at a depth corresponding to a stratigraphic duration of 10 Ma. The attempt was based on the above Equation (1) by assuming several evolution paths. The 10 Ma old horizon was taken as the start of the diagenetic alteration for both the detrital and the authigenic particles, expecting that this may not strictly match the results of the available database. The release of radiogenic ^{40}Ar or the addition of K lowers the ^{40}Ar/^{40}K ratio, and consequently the K-Ar age value, which can be checked by the theoretical but unrealistic closed-system reference (Figure 3, curve 1).

Such behavior is shown for different rate parameters (Figure 3, curves 2, 3, and 4), with a ^{40}Ar release rate similar to that derived in a previous attempt ($\varepsilon \approx 10^{-2}$ Ma^{-1}, [28]) and a K addition rate of the same order of magnitude ($b \approx 10^{-2}$ Ma^{-1}, Table 1).

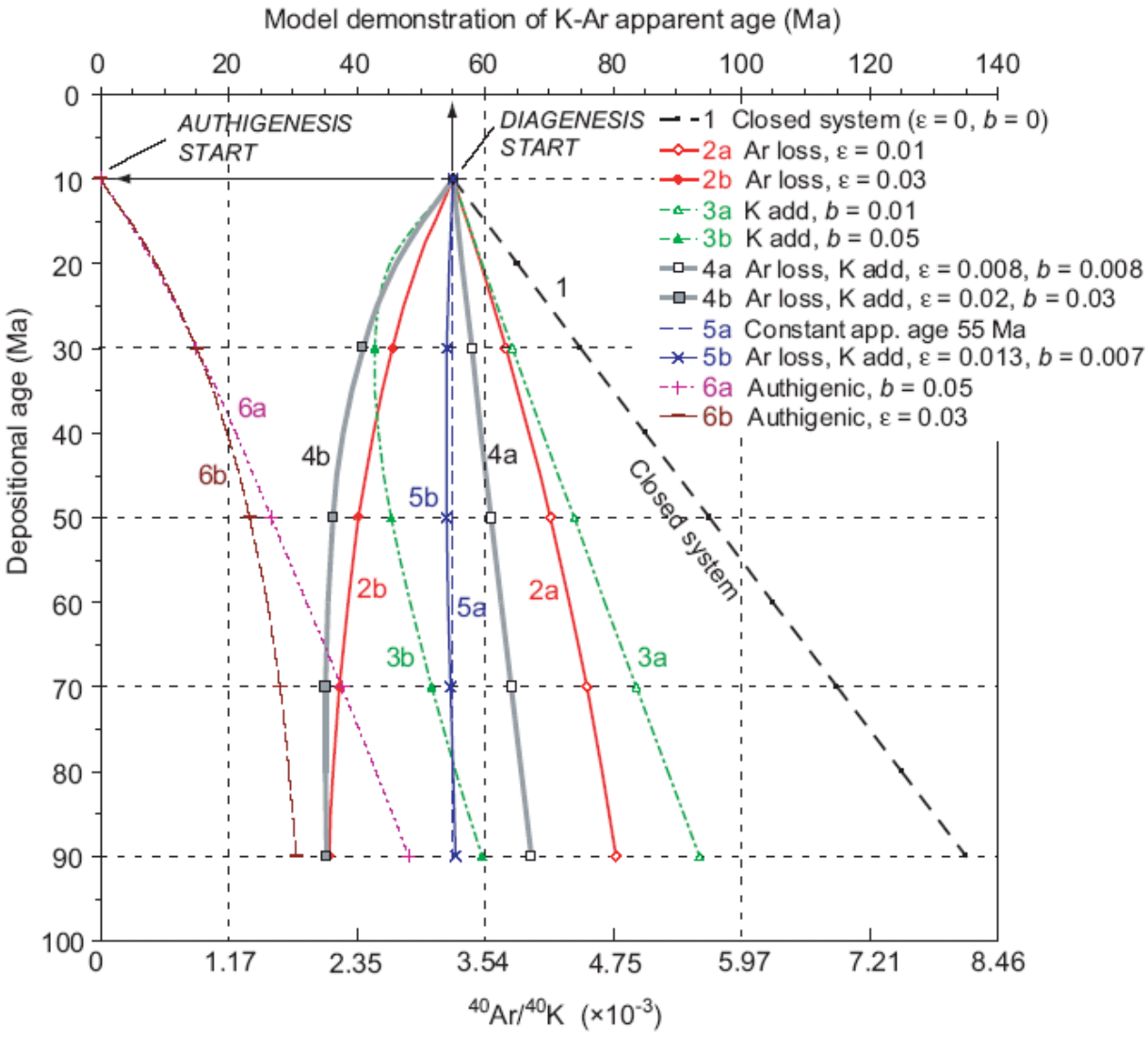

Figure 3. Illustration of the model-calculated changes in the K-Ar apparent ages due to an alteration of 55 Ma old clay particles and a precipitation of newly precipitating crystals of a 0 Ma initial K-Ar age. The increasing depositional age corresponds to increasing sediment burial depth. The theoretical closed system (curve 1) corresponds to no loss or gain of Ar and K. The single process of ^{40}Ar losses (ε, Ma^{-1}) at different rates are shown in curves 2a, b, and that of K gains (b Ma^{-1}) are shown in curves 3a, b. Two processes operating simultaneously at different rates are shown in curves 4a, b. An example of a constant K-Ar apparent age with depth (curve 5a) and its approximation by a two-process model (curve 5b) is shown. Authigenic particles gaining K (curve 6a) or losing ^{40}Ar (curve 6b) with time are also shown. In each case, the increase in the K-Ar apparent age is considerably smaller than if the authigenic particles were a closed system. See the Equation (A4b) in the Appendix A.

Low rates of both ^{40}Ar loss or K addition induce an increase of the K-Ar age from its initial hypothetical value of 55 Ma (Figure 3, curves 2a and 3a), while higher rates of ^{40}Ar loss or K gain (Figure 3, curves 2b and 3b) lead to significant declines in the initial K-Ar age. The model demonstrates changing relationships with a stronger decline in the initial K-Ar age of the particles with higher rates of ^{40}Ar loss than K gain (Figure 3, curves 4a and 4b). A nucleating authigenic illite-type crystal can be assumed to incorporate K

without radiogenic ^{40}Ar when crystallizing and, consequently, with an initial K-Ar age of 0 Ma (Figure 3, curves 6a and 6b). If such a particle continuously gains K, not losing any of the produced ^{40}Ar, its K-Ar age increases with time, as already demonstrated many times. Interestingly, this behavior closely reflects the results obtained for the clay separates of the Mahakam shales, the North Sea section, and the Gulf Coast sequence (Figure 2, curves a, c and d). The clay separates also show nearly constant K-Ar ages within given depth intervals in these sections (Figure 3, curve 5a). Importantly, the combined effect of Ar loss and K uptake operating simultaneously is pronouncedly different from effects of each process operating independently at nearly the same rates (Figure 4, curves 2a and 3a).

Table 1. Summary of stratigraphic data, particle size fractions, K and ^{40}Ar concentration changes for the depositional age intervals as given in the references cited, and the model linear K addition rates (b) and first-order ^{40}Ar release rates (ε).

Location	Approximate Depositional Age (Ma) and Depth Range (m)	Particle Size Fraction	Gain or Loss K Content from Top to Bottom of Section (wt.%)	K Linear Change Rate [e] (%/Ma)	^{40}Ar Linear Change Rate [e] (%/Ma)	This Study:		
						Depositional Age Range (Ma)	Particle Size Fraction	Linear K Increase Rate b, and First-Order ^{40}Ar Release Rate ε (%/Ma)
East Borneo, Mahakam Delta, shales [a]	1(?)–20 Ma 183–4232 m	2–20 µm <0.4 µm total <0.4 µm adjusted [d]	0.74 to 2.42 2.19 to 2.96 3.98 to 4.91	11.3 [f] 1.85 1.22	6.09 −1.17	1(?)–20 Ma 1(?)–8 Ma 8–20 Ma	2–20 µm <0.4 µm <0.4 µm	b = 1, ε = 0.9 (bracketing values: b = from 0.5 to 0.8, ε = from 0.8 to 2) b = 3.5, ε = 3 b = 1, ε = 0.9
Same location, sandstones [a]	1(?)–20 Ma 350–4228 m	2–40, 2–20 µm <0.4 µm total <0.4 µm adjusted [d]	0.76 to 0.35 1.74 to 1.59 3.87 to 6.38	−2.68 −0.45 3.41	−5.26 −4.06	0–20 Ma 1(?)–20 Ma	2–40, 2–20 µm <0.4 µm	From b = −0.6, ε = from 2.5 to b = –1, ε = 2 (bracketing values: b = from −0.7 to −0.5, ε = from 2.0 to 3.3) b = 5, ε = 4 (bracketing values b = from 3 to 5, ε = from 3.5 to 6)
North Sea, Bergen High area, Huldra field [b]	78–190 Ma 2473–4132 m	2–10, 2–15 µm <0.1 µm	1.61 to 4.65 2.56 to 6.13	1.68 1.24	0.60 1.39	70–190 Ma	2–10, 2–15 µm <0.1 µm	bracketing values: b = from 0.2 to 0.3, ε = from 0.5 to 0.7 b = 0.8, ε = 0.7
U.S. Gulf Coast, Harris County, Texas [c]	20–34 Ma 1250–5500 m	whole rock <0.1 µm	2.03 to 3.07 1.88 to 4.02	3.66 high 18–28 8.15	−2.17 2.05	20–34 Ma 26–30 Ma 20–27 Ma 28–34 Ma	whole rock <0.1 µm <0.1 µm	b = from 1.5 to 3, ε = from 2 to 4.5 b = from 15 to 23, ε = from 0 to −3.5 b = 1, ε = 1 b = 2.2, ε = 1

[a] Furlan et al. [24], Clauer et al. [36], [b] Glasmann et al. [22], [c] Aronson and Hower [37], [d] K content adjusted for the presence of detrital minerals, [e] Indicative change from section top to the bottom, increase (+) or decrease (−), [f] Example: (2.422/0.741 − 1)/20 = 11.3.

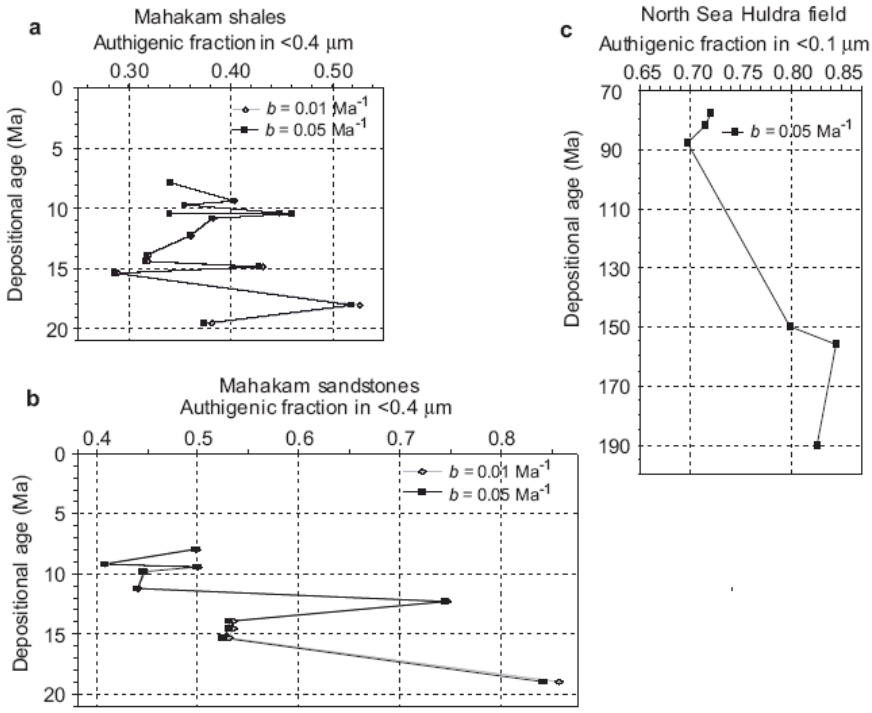

Figure 4. Interpretation of the $^{40}Ar/^{40}K$ ratios and K-Ar apparent ages of fine-grained clay size fractions in the three formations as products of mixing of small-sized particles occurring in the coarse-grained fractions (Figure 1) and the calculated authigenic particles at the same depth in sediment (Figures 5–7) that gain K at the rate b (Ma^{-1}) shown in: (**a**) the Mahakam Delta shales; (**b**) the Mahakam Delta sandstones; (**c**) the North Sea section.

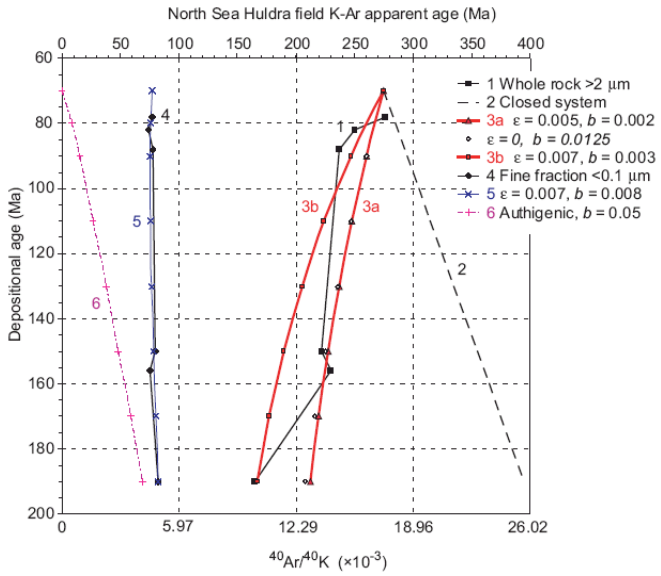

Figure 5. The K-Ar apparent ages of the coarse- (line 1) and fine-grained size (line 6) fractions from the North Sea section [22]. For the coarse-grained fraction: calculated K-Ar dates if the particles were a closed system (line 2); data points bracketed by the two-process model at different rates of ^{40}Ar loss (ε Ma^{-1}) and K gain (b Ma^{-1}) (curves 3a and b); because of a relatively small decrease in the K-Ar apparent age over a long period of time, the two-process curve 3a that shows ^{40}Ar loss and K gain is very close to the one-process result of K gain only (b = 0.0125). For the fine-grained fraction: ^{40}Ar escape and K addition (curve 5) approximate the nearly constant K-Ar apparent age of 77 Ma of the fine-grained fraction. Calculated authigenic particle growth by addition of K (curve 6), starting at depositional age 70 Ma. See Equation (A4b) in the Appendix A.

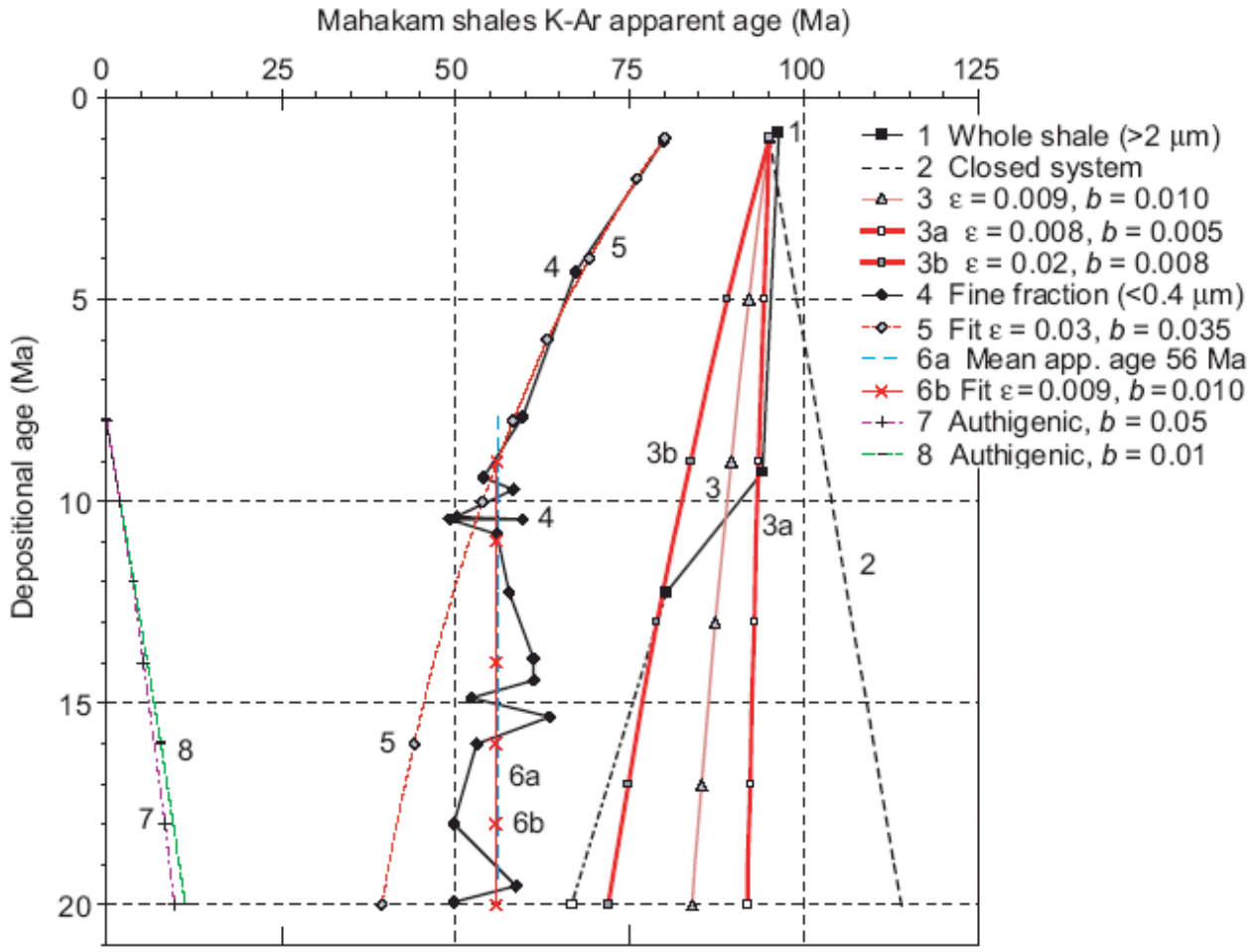

Figure 6. K-Ar apparent age of the coarse- (line 1) and fine-grained (line 4) fractions of the Mahakam shales, calculated from the two-process model of ^{40}Ar loss and K gain at different rates. For the coarse fractions: calculated K-Ar data if the particles were a closed system (line 2); simultaneous ^{40}Ar escape and K addition (bracketing the data points (curves 3a, 3b) and an approximate mean (curve 3). For the fine-grained fractions: depositional age 1–8 Ma, ^{40}Ar escape and K addition (line 5); 8–20 Ma, mean apparent age constant (curve 6a), and the calculated fit for ^{40}Ar escape and K addition (curve 6b). Computed authigenic particles growth by addition of K (curves 7 and 8) at different rates, starting at depositional age 8 Ma. See Equation (A4b) in the Appendix A.

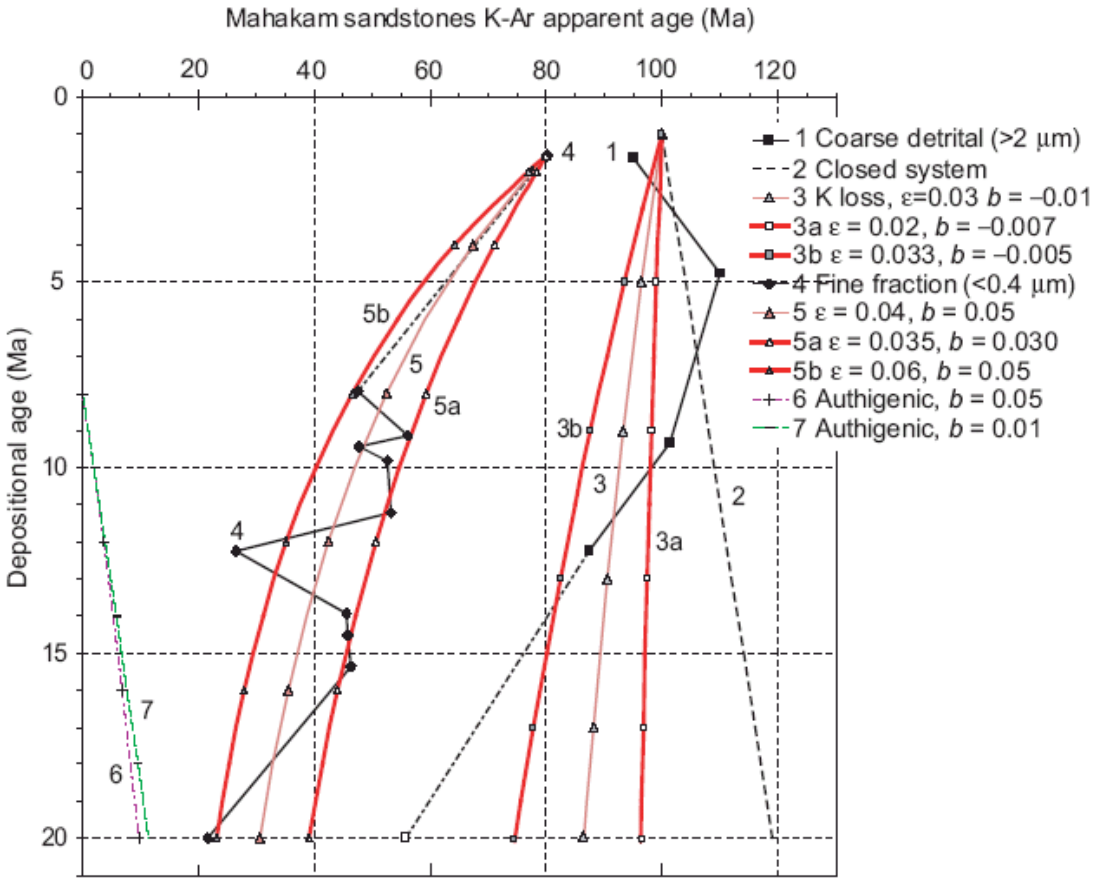

Figure 7. The K-Ar apparent ages of the coarse- (line 1) and fine-grained size fractions (line 4) from Mahakam sandstones. For the coarse fractions, the calculated K-Ar dates of the particles were a closed system (line 2); simultaneous ^{40}Ar escape and K loss (line 3) and approximately bracketing the data points (curves 3a and b). For the fine fractions, the ^{40}Ar escape and K addition (curves 5a, b) approximately bracket the data points and curve 5 is for the middle range. Calculated authigenic particle growth by addition of K at different rates (curves 6 and 7), starting at the depositional age of 8 Ma. See Equation (A4b) in the Appendix A.

6. Mixing of Old Detrital and Young Authigenic Clay Particles

If newly precipitating crystals of an age T_a are mixed with older detrital particles of an age T_d, the age T_{mix} of the mixture will vary as a function of the size of the separates, and will depend strictly, whatever the size of the separate, on the mass fraction x of the newly formed crystals and the mass fraction $1 - x$ of the older crystals in the equation

$$T_{mix} = xT_a + (1 - x)T_d \quad (2)$$

that describes the mean age of the mixture for which each endmember yields its own ^{40}Ar/^{40}K ratios.

Clauer and Chaudhuri [40], Clauer et al. [41] (with references to other publications), and Środoń et al. [47] discussed the K-Ar apparent ages of various mixtures consisting of young authigenic and old detrital particles in fine-grained size fractions (<0.4 µm) of claystones. McCarty et al. [48] also published a mineralogical study of I-S from Gulf Coast sediments, aided by a modeled decomposition of the mineral assemblage that shows that the nucleation of smectite-rich particles occurred on the surface of detrital crystals or grains and not in the interlayer sites of the already present detrital sheet silicates. This strongly suggests that authigenesis of I-S crystals is independent from alteration of the co-existing detrital material, except if the reaction is a complete dissolution of the detritus followed by a related crystallization of new I-S, for which no evidence is visible in the

three case studies examined here. The fractions x of the authigenic crystals computed from Equation (2) are shown for the Mahakam and the North Sea sediments (Figure 4). The K-Ar ages of the fine-grained size fractions from these two sequences (Figure 3, curves a, b and c) combine an authigenic nucleation and growth of new crystals mixed with the smallest detrital particles, as a weighted mean age T_{mix} of the fine-grained fractions. This interpretation is based on the fact that authigenic I-S starts to form in its sedimentary environment sometime after deposition and that it changes into illite during progressive temperature increase due to burial possibly associated with a greater availability of K. In addition, the detrital components of the sediment also contain small-sized crystals of T_d K-Ar apparent ages similar to those of the coarse-grained detrital material. Although the impact of an authigenic crystallization on the K-Ar system of sedimentary I-S has been extensively documented (e.g., discussion in [4]), with references to other studies and more since), no data, as far as we are aware of, either confirm or negate the occurrence of small-sized detrital crystals with strictly the same age as the coarse-grained detrital counterparts. In fact, small crystals in claystone often yield younger K-Ar apparent ages than the large fractions, probably compiling more extensively the alteration/weathering that favored larger releases of radiogenic ^{40}Ar. This does not distract from the fact that the smaller size fractions also contain more authigenic crystals than the coarser grained fractions.

The above mixing Equation (2) is based on two essentials: (1) authigenic crystals that are assumed to form by continuous addition of K at a linear rate from 1 to 5%/Ma (b = 0.01 to 0.05 Ma^{-1}), and (2) produced radiogenic ^{40}Ar stored with changes in the K-Ar age values depending on the relative increases of both. The $^{40}Ar/^{40}K$ ratios and their associated K-Ar apparent ages decrease with depth in the coarser grained fractions, most probably because of a preferential release of ^{40}Ar. The mixing model can be demonstrated, at its simplest, by the data of the North Sea sequence (Figure 4, curve c, [22]). The K-Ar ages of the coarse-grained, mostly detrital fraction (T_d, Figure 5, curve 1) and the calculated K-Ar age of the authigenic fraction (T_a, Figure 5, curve 6) for a starting authigenesis at 70 Ma were used in Equation (2) with the true T_{mix} age of the fine-grained < 0.1 µm fraction (Figure 5, curve 4), to obtain the mass fraction x of the authigenic material in the mixture. In turn, the results of the two-process model depend on the K addition rate to the authigenic crystals, that is to say, in turn on how fast the authigenic particles grew.

The example of the Mahakam Delta provides another interesting aspect with its very short and recent deposition time between 20 and 0 Ma (Figure 2, curves a and b), which are both much lower and shorter than for the two other sections (Figure 2, curve c). The Mahakam Basin is still an active receiver with a present-day river delta at the top of the sedimentary sequence in an almost unchanged drainage basin since 20 Ma. In the shales of the sequence, the K-Ar apparent ages of the fine-grained clay size fraction decrease from 80 Ma at the surface to about 56 Ma near a depth of 2000 m, and the average below this remain approximately constant around those of 56 Ma until a depth of 4200 m. Approximately 8 Ma after deposition, the trend of the K-Ar ages changes at a depth of about 2000 m, becoming constant after a continuous decrease. The addition of the authigenic mass fraction x was estimated on the basis of the T_{mix} K-Ar apparent age of the <0.4 µm fraction within a deposition interval from 8 to 20 Ma given by the analytical data (Figure 2a or Figure 6, curve 4) and the K-Ar apparent ages T_d of the coarse-grained fraction given by the calculated trend of the data (Figure 6, curve 3). This limited K increase in the coarser grained size fraction, as shown by the analytical data of the shales from the three sequences (Table 1), implies crystallization of authigenic crystals also in the coarse-grained fractions, which could have resulted from a nucleation of small crystals growing rapidly on larger detrital particles, as suggested in the previous section. The calculated K-Ar ages of the authigenic fraction are also shown (Figure 5, curve 7 for a linear K addition rate b = 0.05 Ma^{-1} and curve 8 for the same rate b = 0.01 Ma^{-1}). During the relatively short deposition time of 12 Ma, the calculated K-Ar ages of the authigenic fractions appear to be similar. The consequence is that the lower the b Ma^{-1} rate of the K gain is, the closer the K-Ar ages are to those of a closed system. The authigenic mass fraction x increases

irregularly down the sedimentary sequence from about 35% to near 50% of the mixtures (Figure 4a). In the sandstones of the Mahakam Basin (Figure 2b), the K-Ar apparent age trend of the <0.4 μm size fraction is different from that of the shales, consisting mostly of detrital material and decreasing continuously from about 55 Ma at the deposition time to about 20 Ma at a depth of 4000 m. The mass fraction of the <0.4 μm authigenic particles (Figure 4b) that is computed similar to that of the shales, increases from about 45% to 85% over the same 12 Ma period of deposition. This substantial increase could result from an extended dissolution of coarse-grained detrital grains that potentially induce a greater ^{40}Ar loss and more K available for a concomitant illitization portraying a stronger diagenesis in the sandstones than in the shales, which was already described analytically [16,38].

Since the calculated authigenic mass (x) depends on the assumed rate of K addition to the authigenic particles (b) that gives their K-Ar age T_a in Equation (2), its limiting effects on the mass need to be briefly discussed. If the authigenic particles would grow as a closed system (b = 0), their K-Ar age T_a would be necessarily greater than in the case of a continuous addition of K, and their mass fraction x in the mixture would be larger. Beyond the fact that the closed system is only a theoretical reference case, this condition would hold only as long as the K-Ar ages of the authigenic crystals do not exceed those of the fine-grained fractions ($T_a \leq T_{mix}$). If the K addition rate to the authigenic crystals is high, their K-Ar age would be low, and at the limit of $T_a \approx 0$, the mass fraction x would be smaller than the values calculated for the finer grained clay fractions in the cases of the Mahakam and North Sea sections. This would represent a lower limit for the authigenic part in mixed fractions.

7. A Comparison between the Analytical Results and the Modeled Data

The two-process model does not address the analytical variations of the individual data points that may relate to poorly known factors, such as the variability of the ^{40}Ar/^{40}K initial values at the time of deposition, progressive changes of the diagenetic regime in a thick sediment column, or abrupt changes of rock characteristics such as the porosity or the permeability. Moreover, the estimated loss of radiogenic ^{40}Ar with increasing sediment depth is not based strictly on its concentration in the clay crystals, but represents the deficit of ^{40}Ar in a crystal of a certain K-Ar age relative to the age that the crystal would have, if its ^{40}Ar would have grown in a closed system, which may be a fair approximation. Thus, various ^{40}Ar/^{40}K values for scattered data points of clay separates at the time of deposition are plausible, providing K-Ar apparent age trends relative to the youngest analytical data point of each. Therefore, the rates of K addition and Ar release estimated by the two-process model are mean rates for each size fraction that contains mixtures, while not applying separately to the authigenic or the detrital crystals of each size fraction. The model equations are given in the Appendix A.

7.1. In the Coarse-Grained Size Fractions

Despite their wide scatter, the K-Ar apparent ages of coarse-grained size fractions from selected sequences can be simulated by the two-process model, with a first-order ^{40}Ar release (ε Ma^{-1}) from a K uptake by the crystals of different initial K-Ar apparent ages (Figure 7, curve 3 and bracketing curves 3a and b; Figure 8, curves 3a and b). Most of the studied coarse-grained size fractions yield an increase in the K content with increasing depth (Table 1) and a correlative decrease in the associated K-Ar ages. Only the coarse-grained fractions of the Mahakam sandstones, but not of the shales, show a decrease in the K content with depth (Table 1), their analytical data being bracketed by the model that describes simultaneously a combined ^{40}Ar and K loss.

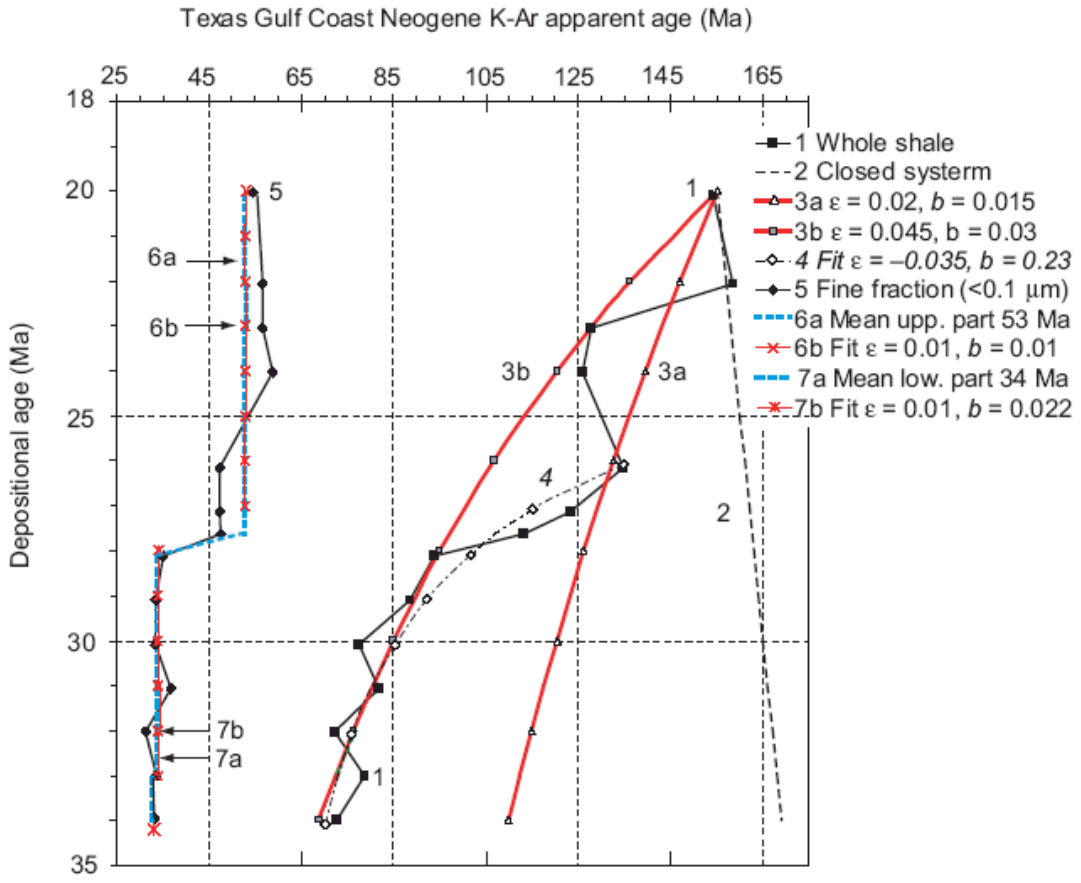

Figure 8. The K-Ar apparent ages of the coarse- (line 1) and fine-grained size fractions (line 5) of the Gulf Coast sequence [37]. For the coarse-grained fraction: calculated K-Ar dates if the particles were a closed system (line 2); data points approximately bracketed by the two-process model of ^{40}Ar escape (ε Ma^{-1}) and K addition (b Ma^{-1}) at different rates. The abrupt change in the decline of the K-Ar date at the depositional age of about 26 Ma in the sediment is simulated (curve 4) by addition of K at a fast rate of b = 0.15 Ma^{-1} without ^{40}Ar escape (ε = 0). For the fine-grained fraction: data points between 20 Ma and 27 Ma approximated by a constant K-Ar apparent age of 53 Ma (line 6a); the data point between 28 Ma and 34 Ma, constant apparent age of 34 Ma (line 7a). The latter two straight-line segments approximated by the model of ^{40}Ar release and K addition at relatively low rates (curves 6b and 7b). See Equation (A4b) in the Appendix A.

The K-Ar ages of the whole rocks from the Gulf Coast sequence (Figure 8, curve 1) probably indicate a change in the diagenetic regime near the 26 Ma stratigraphic age, which is supported by the changing trend of the K-Ar ages from the fine-grained fractions (Figure 1d). During deposition between 26 and 34 Ma, the K concentration of the shales increases strongly between 3100 m and 4000–4300 m at a linear rate b = 18 to 28%/Ma. The K-Ar ages of the lower part of the shale whole-rock data (Figure 8, curve 4) yield a range of K gain rates from b = 23%/Ma to b = 15%/Ma and ^{40}Ar loss rates from ε = −3.5%/Ma to ε = 0 (not shown). Interestingly, this estimation agrees with the conclusions of Aronson and Hower [37] about the K gain by the shales (Table 1).

The sensitivity of the two-process model is demonstrated by the differences in the calculated K-Ar ages produced by variations of about one order of magnitude in the ^{40}Ar release rate ε (0.5 to 4.5%/Ma) and a similar variation in the K gain rate b (0.2 to 3%/Ma), each varying around a value of about 1%/Ma.

7.2. In the Fine-Grained Size Fractions

The fine-grained clay minerals of the three studied sections all yield increased K contents with depth (Figure 1 and Table 1) and a correlative increase in the abundance of illite forming from I-S. However, the trends of the K-Ar apparent ages differ considerably from one stratigraphic section to another. According to the two-process model, these trends correspond to significantly various rates of the individual processes in the different sections. The stratigraphic age interval of 8 Ma for the upper Mahakam shales (Figure 5) and that of 20 Ma for the entire Mahakam sandstones section (Figure 6) show a pronounced, although fluctuating, decrease in the K-Ar ages with depth. These fluctuations probably integrate local variations of the ratio among the authigenic and detrital materials in the size fractions with various sources for the detrital supply. The limited fluctuations are not taken into consideration in the model as they obscure the general trends that can be bracketed with the rate parameters ε and b higher than those in the simulations for the coarse-grained fraction (Figures 5 and 6, curve 4). For instance, the decrease in the K-Ar apparent ages within the upper sections of the two Mahakam profiles, during the deposition time from 1 to 8 Ma, refers either to a ^{40}Ar loss of about 40% for the mixed detrital and authigenic material ($\varepsilon = 0.06$ Ma^{-1}, b = 0) or, more probably as discussed earlier, to a combination of about 20% of ^{40}Ar lost and 25% of ^{40}K addition to the crystals in the considered time interval of 8 Ma ($\varepsilon = 0.03$, b = 0.035 Ma^{-1}).

The lower Mahakam shale section, during the deposition time from 8 to 20 Ma, and the North Sea section with a considerably longer deposition interval from 80 to 190 Ma, both provide K-Ar apparent ages that appear approximately constant with depth (Figure 5, curve 6a, and Figure 7, curve 6). Little or no changes in the ^{40}Ar/^{40}K ratio or in the K-Ar ages require a mechanism that counterbalances the natural increase in ^{40}Ar due to the ^{40}K decay and the natural ^{40}Ar decrease lost by the altered detrital crystals. The two-process model provides a good fit for the data of the Mahakam shales (Figure 5, curve 6b) and of the North Sea section (Figure 7, curve 5), with rates for the ^{40}Ar release rate (ε) and the K addition (b) considerably lower than in the other sections where the K-Ar ages change fast and scatter widely. This suggests that a continuing illitization/alteration process in shales may depend less on the absolute or relative increase in K than on the extent of in situ mineral reactions.

The small-sized clays of the Gulf Coast sequence (Figure 8, curves 6a and 7a) show two or possibly three step-like decreases in the K-Ar age values relative to depth. Aronson and Hower [36] reported an increase in K (Figure 1d) and in illite-type crystals of the finer grained clay fraction with increasing depth. However, the reasons for the relatively abrupt declines in the K-Ar ages are still not clear; a progressive increase in temperature due to increasing depth, as suggested by those authors, should not provide the observed abrupt change, unless a discrete tectonic-thermal event occurred at the time. Odin [49] for Fe-rich glauconite crystals and Eberl [37] for illite-type crystals launched the idea that these steps could result from a sudden change in the physical-chemical conditions of the progressively burial-induced diagenesis, such as the just mentioned supplementary tectonic-thermic event. In fact, to remain "sealed" in a sequence that continues to be buried, clay particles crystallizing during such a "punctuated" event have to had been crystallized within an environment characterized by higher temperatures and/or in contact with fluids with a chemical composition different than usual at the given depth, so that their K-Ar system would remain unchanged when buried deeper. There were no temperature variations that were obvious in the Gulf Coast sequence to support a spontaneous "abnormal" temperature variation, therefore, it cannot be denied that the pore-fluid chemistry might have changed for a time. In addition, a pronounced uptake of K should have induced an even more significant decrease in the K-Ar apparent ages than that observed in the deeper section between 3000 and 4000 m. In the two-process model, each of the corresponding segments can be well approximated with the ^{40}Ar release rate of $\varepsilon = 0.010$ Ma^{-1} and the K addition rate of b = from 0.010 to 0.022 Ma^{-1}. The similar K-Ar age trends in the Mahakam shales, the North Sea section, and the Gulf Coast sequence consolidate the fact that, based on an

addition of K to the clays starting a few to a few tens of Ma after deposition, illitization is accompanied by a loss of radiogenic ^{40}Ar and probably of K from nearby or even intergrown detrital K-bearing minerals.

8. Contribution of the Model to the Current Knowledge of the Illitization Process

By comparing the K-Ar apparent ages of fine-grained sized separates consisting of both detrital and authigenic illite-type particles from the three selected basins, Clauer and Chaudhuri [27] showed that radiogenic ^{40}Ar in illite-type minerals was retained preferentially in the zones of intense illitization, where one would expect it to escape spontaneously in the course of mineral reactions involving K addition. Those authors also observed that illitization of I-S in shales was controlled by the dissolution of other present detrital components, such as feldspar grains and biotite flakes, mainly in the deeper part of the Mahakam Basin [24]. The fact that illitization begins in the upper part of sedimentary basins, such as here in the Gulf Coast and the Mahakam Basins with the classical S-shaped curve of illite increase relative to depth, suggests a K uptake downwards (Figure 1d). By contrast, even if the radiogenic ^{40}Ar released from detrital components is notably less constrained analytically, some of the radiogenic ^{40}Ar of the detrital and authigenic mixture had to diffuse out of the crystals when the host rocks were buried deeper, as its sole accumulation steadily increases the K-Ar ages by decay down the sediment sequences. As this is visibly not the case, it is a need to speculate about a mixture of particles that mainly increase their K content and particles that release radiogenic ^{40}Ar with K in various proportions depending on their alteration state. Such a two-process model allows dealing with this contradictory aspect, as it shows which process is dominant and when, and consequently how, and at which depths the authigenic and detrital components contribute to the K-Ar apparent ages of clay-rich size fractions.

The K-Ar age trends of the shales from the three studied basins, match the two-process model if the rates of K addition and radiogenic ^{40}Ar release are adjusted to each specific history. For the decrease in the K-Ar ages from upper shales and sandstones of the Mahakam Basin, the model allows a choice between a ^{40}Ar loss of about 40% of the initial content and the amount produced since deposition, or a combination of about 20% ^{40}Ar loss and 25% ^{40}K addition to the particles, which appears to fit well with the available analytical results. These estimates are within the range of the analytical K-Ar results, and they bracket the K-Ar analytical trend. The two-process model also provides a good fit for the data, even when the K-Ar analytical trends change, meaning, in turn, that the model has a wide potential application. This is the case for the Mahakam shales, where the ^{40}Ar release (ε) and the K addition (b) rates are considerably lower in the deeper section relative to sections where the K-Ar ages changed fast. It also suggests that a continuing illitization in some shales below a given depth depends less on the addition of K from outside than on in situ mineral reactions.

As mentioned earlier, the quite systematic mixing of authigenic and detrital clay materials in deeper shales can provide nearly constant K-Ar ages for clay mixtures [27]. A strict steady-state behavior has no scientific reality from what was already discussed, and altogether it would be unlikely attained at the relatively short time scale that frames the evolution in the three studied basins [38]. In the Mahakam shales where the fine-grained clay minerals yield an almost constant K-Ar record at a depth between 2000 and 4000 m, the average amount of the small-sized authigenic clay materials increases only slightly from 34% in the upper section to 38% in the lower section, with extreme values at 29% and 52%. In the North Sea section, the amount of authigenic clay crystals of the fine-grained shallow fractions also increases in the same K-Ar age range, again only slightly from 72% in the upper section to 83% in the deeper section, with extreme values scattered from 70 to 84%. The limited increase in the small-sized authigenic contents indirectly records limited diagenetic activity, while the wide data scatter is suggestive of variable K additions and radiogenic ^{40}Ar releases that may depend on specific local parameters of the rocks. Such wide and rapid changes could correspond to abrupt changes in the porosity/permeability

of the rocks, the fluid pressure, and/or the K availability. The varied provenance of the particles also potentially increases the scatter of the initial $^{40}Ar/^{40}K$ ratios, which adds to the initial dispersion. However, such processes do not negate the main trend of the observed lowering of the K-Ar apparent ages with increasing depth, accompanied by an increase in the amount of authigenic material and a higher decrease of radiogenic ^{40}Ar.

In fact, some of the K trends show a more or less continuous increase in the deeper sections, such as in the North Sea (Figure 1c), but some also show intervals with rapid increases, such as in the Gulf Coast (Figure 1d) where the K content of the fine-grained clay fraction doubles over about 3 Ma, which relates consistently with the mineralogical data, with a drop in the K-Ar age of about 35%. The same depth interval is also characterized by a strong K increase of the coarse-grained fraction (Figure 8, curve 1) that has been recalculated as a linear rate of b = from 0.18 to 0.28 Ma^{-1} and modeled at a value of b = from 0.15 to 0.23 Ma^{-1}. These are among the highest rates of K gain in the sections studied here (Table 1). In the case of decreasing K-Ar apparent ages, the representation of radiogenic ^{40}Ar gives a characteristic picture of the system because ^{40}Ar is continuously produced in any of the particles at strictly the same rhythm. However, high rates of K gain in parts of the sedimentary section that are at least 10 times higher than the rates derived from the two-process model would require addition of ^{40}Ar to the particles ($\varepsilon < 0$) to simulate the data trend. It is difficult to account for such a theoretical mechanism in any interval of the examined stratigraphic sections (Figure 7, curve 4), unless the authigenic particles also incorporate radiogenic ^{40}Ar when crystallizing, which can only be a process with a limited impact, as previously discussed.

In summary, the model can closely simulate changes in the K-Ar apparent ages of coarse- and fine-grained clay fractions, relative to either deposition time or burial depth. It simulates changing fluxes of ^{40}Ar escape from and K addition to the crystals of different sizes along stratigraphic sedimentary intervals. The two-process model also explains the nearly constant $^{40}Ar/^{40}K$ ratio in the clay fractions of shales from deeper stratigraphic intervals resulting from lower rates of K addition and ^{40}Ar release (b and ε each about 1%/Ma or 0.01 Ma^{-1}). Therefore, they provide a realistic alternative explanation to the non-realistic steady state situation with respect to the $^{40}Ar/^{40}K$ ratio of progressively buried sediments. It allows extraction of values for the changing K addition and radiogenic ^{40}Ar release during burial of varied types of rock sequences.

9. Conclusions

For a long time, it has been known that clay diagenesis corresponds mainly to illitization of smectite and illite/smectite mixed layers in sedimentary sequences that is usually accompanied by changes in the $^{40}Ar/^{40}K$ ratio and the K-Ar ages of various size fractions. Commonly, sedimentary size fractions have K-Ar apparent ages older than the stratigraphic reference, especially in the case of shales. Although Ar is not a constituent of the stoichiometric formula of K-bearing clays, its ubiquitous occurrence in such minerals makes it a useful tracer of diagenetic illitization through the metric of their K-Ar apparent ages. A systematic decrease in the $^{40}Ar/^{40}K$ ratios and in the associated K-Ar ages of clay-rich size fractions with increasing depth or increasing burial time relates to: (1) the addition of K into newly forming authigenic particles that mix with and progressively take over the detrital particles when depth increases, (2) the release of radiogenic ^{40}Ar from detrital particles that are progressively altered by burial-driven changes, or (3) more commonly, a combination of the two processes operating simultaneously but independently.

The previously published K-Ar apparent ages of coarse- (mainly >2 μm) and fine-grained (mainly < 0.4 μm) size fractions of the Neogene shales and sandstones of the Mahakam Delta in Eastern Borneo, the Early Jurassic-Late Cretaceous section of the North Sea, and the Late Oligocene-Early Miocene sequence in the Texas Gulf Coast were detailed and modeled. The different size fractions represent mixtures of older detrital particles with younger, newly formed authigenic crystals. As a result, the mass fraction of the authigenic particles in the fine-grained clays is generally increasing with buried sediments owing to

an increase with time of the calculated $^{40}Ar/^{40}K$ ratio in the authigenic particles and a variable decrease of the $^{40}Ar/^{40}K$ ratio in the detrital fraction.

The conceptual model, developed in this study, describes how the $^{40}Ar/^{40}K$ ratios and K-Ar apparent ages depend on two processes operating simultaneously but independently, i.e., an addition of K to the particles at a linear rate b Ma^{-1} and a release of radiogenic ^{40}Ar from other crystals by a first-order flux with a constant ε Ma^{-1} rate. The estimated rates are mean values of a model simulating the changes with burial depth or deposition time in the K-Ar apparent ages of the various clay fractions, starting with a $^{40}Ar/^{40}K$ value representative of the particles at the time of deposition. The analyzed decrease with depth of the K-Ar ages from coarse-grained fractions (>2 μm) is bracketed by a ^{40}Ar escape rate ε in a range from 0.5 to 4.5%/Ma (ε = from 0.005 to 0.045 Ma^{-1}), by a K gain rate b in a range from 0.2 to 3%/Ma (b = from 0.002 to 0.03 Ma^{-1}) and by a K loss rate of b = –0.01 Ma^{-1} in the Mahakam sandstones. In the corresponding Mahakam shales, as well as the North Sea and the Texas Gulf Coast shale sections, the fine-grained fractions are characterized by K-Ar apparent ages that are nearly constant with depth, despite some scatters of the data. The two-process model simulates a nearly constant $^{40}Ar/^{40}K$ ratio with depth resulting from lower rates of K addition and ^{40}Ar release (b and ε each about 1%/Ma or 0.01 Ma^{-1}). It confirms that no change in the K-Ar apparent ages of the fine-grained clays with increasing stratigraphic depth does not represent a steady state with respect to $^{40}Ar/^{40}K$ in a sedimentary sequence, but is part of a continuing but changing illitization at a slower rate.

The rates of K addition and Ar release control the decrease in the K-Ar ages of clay mixtures with increasing depth in the sediments. Although illitization induced by burial requires the addition of K to clays, the process as a whole is a combination of a simultaneous release of radiogenic ^{40}Ar from and an addition of K to sized mixtures of authigenic and detrital particles. However, the lower rates of K gain and Ar release that simulate the sections with near-constant K-Ar ages in the shales of the three studied locations below a certain depth suggest that a continuing illitization in some geologic settings depends less on the addition of K than on in situ mineral reactions.

Author Contributions: Conceptualization: N.C.; methodology: A.L.; software: A.L.; validation: N.C.; writing original draft: N.C.; writing review: A.L. and N.C. All authors have read and agreed to the published version of the manuscript.

Funding: The authors received no external funding.

Data Availability Statement: Data available upon request.

Acknowledgments: This research was supported by the Arthur L. Howland Fund of the Department of Earth and Planetary Sciences, Northwestern University and by ANDRA (Agence Nationale pour la gestion des Déchets RAdioactifs). We would also like to extend our personal thanks to Dr. T. Uysal of the University of Queensland who very kindly accepted to comment on the initial version of this script.

Conflicts of Interest: The authors declare no conflict of interest.

Appendix A. $^{40}Ar/^{40}K$ Atomic Ratio and K-Ar Apparent Age in Open and Closed Systems

1. Closed system: production of radiogenic ^{40}Ar from ^{40}K, no K or ^{40}Ar addition or loss

^{40}Ar is produced by the decay of ^{40}K, as given in a well-known equation (e.g., [26]):

$$d(^{40}Ar)/dt = \lambda_a {}^{40}K_0 e^{-\lambda t}, \quad \text{(A1a)}$$

where $\lambda_a = 0.581 \times 10^{-4}$ Ma^{-1} is the decay rate constant of ^{40}K to ^{40}Ar, and $\lambda = 5.543 \times 10^{-4}$ Ma^{-1} is the total decay rate constant of ^{40}K to ^{40}Ar and ^{40}Ca. The concentration units of ^{40}Ar and ^{40}K are mol/g.

If no ^{40}Ar is present initially in the particles, at time t = 0, then the solution of Equation (A1a) is:

$$\frac{^{40}\mathrm{Ar}}{^{40}\mathrm{K}} = \frac{\lambda_a}{\lambda}(e^{\lambda t} - 1) \quad \text{(A1b)}$$

^{40}Ar and ^{40}K are present initially at time $t = \tau$, where the isotope ratio is $(^{40}\mathrm{Ar}/^{40}\mathrm{K})_\tau$:

$$\frac{^{40}\mathrm{Ar}}{^{40}\mathrm{K}} = \frac{\lambda_a}{\lambda}(e^{\lambda(t-\tau)} - 1) + \left(\frac{^{40}\mathrm{Ar}}{^{40}\mathrm{K}}\right)_\tau e^{\lambda(t-\tau)} \quad \text{(A1c)}$$

Apparent age = (t_{app})

When no ^{40}Ar is present initially in the particles, the apparent age is from Equation (A1b):

$$t_{app} = \frac{1}{\lambda}\ \ln\left(1 + \frac{\lambda}{\lambda_a} \cdot \frac{^{40}\mathrm{Ar}}{^{40}\mathrm{K}}\right) \text{ (with } \lambda \text{ and } \lambda_a \text{ are in units of } \mathrm{Ma}^{-1}) \quad \text{(A1d)}$$

When ^{40}Ar is present initially, $(^{40}\mathrm{Ar}/^{40}\mathrm{K})_0$, the apparent age is from Equation (A1c):

$$t_{app} = \frac{1}{\lambda}\ \ln\frac{^{40}\mathrm{Ar}/^{40}\mathrm{K} + \lambda_a/\lambda}{(^{40}\mathrm{Ar}/^{40}\mathrm{K})_0 + \lambda_a/\lambda} \quad \text{(A1e)}$$

2. Open system: production of ^{40}Ar from ^{40}K and simultaneous loss of ^{40}Ar at a rate ε

Mass balance equation:

$$\underset{^{40}\mathrm{Ar\ growth}}{d(^{40}\mathrm{Ar})/d\mathrm{t} = \lambda_a {}^{40}\mathrm{K}_0 e^{-\lambda t}} \underset{^{40}\mathrm{Ar\ escape}}{- \varepsilon(^{40}\mathrm{Ar})} \quad \text{(A2a)}$$

where λ_a and λ are the decay rate constants as defined above, and ε is a first-order rate constant (in units of yr^{-1}) for the release of ^{40}Ar from the particles.

When there is no ^{40}Ar in the particles initially (^{40}Ar/^{40}K = 0 at time t = 0), the solution is [38]:

$$^{40}\mathrm{Ar}/^{40}\mathrm{K} = \lambda_a\ [1 - e^{-(\varepsilon\ -\ \lambda)t}]/(\varepsilon - \lambda) \quad \text{(A2b)}$$

When ^{40}Ar is initially present, at time $t = \tau$, the isotope ratio is $(^{40}\mathrm{Ar}/^{40}\mathrm{K})_\tau$, and the solution is:

$$\frac{^{40}\mathrm{Ar}}{^{40}\mathrm{K}} = \frac{\lambda_a}{\varepsilon - \lambda}\left[1 - e^{-(\varepsilon-\lambda)(t-\tau)}\right] + \left(\frac{^{40}\mathrm{Ar}}{^{40}\mathrm{K}}\right)_\tau e^{-(\varepsilon-\lambda)(t-\tau)} \quad \text{(A2c)}$$

CHECK: When no ^{40}Ar escapes, ε = 0, and Equation (A2c) becomes identical to Equation (A1c) for a closed system.

3. Open system:

(a) Addition of K to particles at a linear rate b, production of ^{40}Ar without loss

$$\underset{\text{K addition, } ^{40}\mathrm{Ar\ growth}}{d(^{40}\mathrm{Ar})/d\mathrm{t} = \lambda_a {}^{40}\mathrm{K}_0(1 + bt)e^{-\lambda t}} \quad \text{(A3a)}$$

When there is no ^{40}Ar in the particles initially (^{40}Ar/^{40}K = 0 at time t = 0), the solution is [16]:

$$\frac{^{40}\mathrm{Ar}}{^{40}\mathrm{K}} = \frac{\lambda_a}{\lambda(1 + bt)}\left[\left(1 + \frac{b}{\lambda}\right)e^{\lambda t} - \left(1 + bt + \frac{b}{\lambda}\right)\right] \quad \text{(A3b)}$$

When ^{40}Ar is initially present, at time t = 0, the initial isotope ratio is $(^{40}\mathrm{Ar}/^{40}\mathrm{K})_0$, and the solution is:

$$\frac{^{40}\mathrm{Ar}}{^{40}\mathrm{K}} = \frac{\lambda_a}{\lambda(1 + bt)}\left[\left(1 + \frac{b}{\lambda}\right)e^{\lambda t} - \left(1 + bt + \frac{b}{\lambda}\right)\right] + \left(\frac{^{40}\mathrm{Ar}}{^{40}\mathrm{K}}\right)_0 \frac{e^{\lambda t}}{1 + bt} \quad \text{(A3c)}$$

CHECK: In the preceding, when there is no K addition, $b = 0$, and the equation becomes identical to that for a closed system, Equation (A1c).

(b) Addition of K to particles at an exponential rate b, production of ^{40}Ar without loss

$$d(^{40}\mathrm{Ar})/d\mathrm{t} = \lambda_a {}^{40}\mathrm{K}_0 e^{b\mathrm{t}} e^{-\lambda t} = \lambda_a {}^{40}\mathrm{K}_0 e^{(b\text{-}\lambda)t} \quad \text{(A3d)}$$

K addition, ^{40}Ar growth

The solution of Equation (A3d), with an initial $(^{40}\mathrm{Ar}/^{40}\mathrm{K})_\tau$ ratio at time $t = \tau$, is similar to the case of ^{40}Ar escape only, as given in Equation (A2c):

$$\frac{^{40}\mathrm{Ar}}{^{40}\mathrm{K}} = \frac{\lambda_a}{b-\lambda}\left[1 - e^{-(b-\lambda)(t-\tau)}\right] + \left(\frac{^{40}\mathrm{Ar}}{^{40}\mathrm{K}}\right)_\tau e^{-(b-\lambda)(t-\tau)} \quad \text{(A3e)}$$

4. Open system:

(a) Addition of K to particles (linear rate b) and ^{40}Ar release (first-order rate parameter ε) Mass-balance equation:

$$d(^{40}\mathrm{Ar})/dt = \lambda_a {}^{40}\mathrm{K}_0(1{+}bt)e^{-\lambda t} - \varepsilon(^{40}\mathrm{Ar}) \quad \text{(A4a)}$$

K addition ^{40}Ar growth ^{40}Ar escape

The process starts at time $t = 0$ and the initial ^{40}Ar/^{40}K ratio is $(^{40}\mathrm{Ar}/^{40}\mathrm{K})_0$. Solution of Equation (A4a) is:

$$\frac{^{40}\mathrm{Ar}}{^{40}\mathrm{K}} = \frac{\lambda_a}{(\varepsilon-\lambda)(1+bt)}\left[\left(\frac{b}{\varepsilon-\lambda} - 1\right)e^{-(\varepsilon-\lambda)t} + 1 + bt - \frac{b}{\varepsilon-\lambda}\right] + \left(\frac{^{40}\mathrm{Ar}}{^{40}\mathrm{K}}\right)_0 \frac{e^{-(\varepsilon-\lambda)t}}{1+bt} \quad \text{(A4b)}$$

CHECK: When no ^{40}Ar escapes from the particles, $\varepsilon = 0$, and Equation (A4b) becomes identical to Equation (A3c); when no K is added to the particles, $b = 0$, and Equation (A4b) becomes identical to Equation (A2c); with both ε and b equal to 0, Equation (A4b) becomes an equation for a closed system, Equation (A1c).

A special case may be when the ^{40}Ar/^{40}K ratio and the K-Ar apparent age are approximately constant with depth, such that the K-Ar apparent age does not change as the depositional age of sediment (its stratigraphic age) increases with depth. This condition corresponds to:

$$^{40}\mathrm{Ar}/^{40}\mathrm{K} \approx (^{40}\mathrm{Ar}/^{40}\mathrm{K})_0 \quad \text{(A4c)}$$

The preceding equality is used in Equation (A4b), to give:

$$\frac{^{40}\mathrm{Ar}}{^{40}\mathrm{K}} = \frac{\lambda_a}{\varepsilon-\lambda}\left[1 - \frac{b}{\varepsilon-\lambda}\cdot\frac{1-e^{-(\varepsilon-\lambda)t}}{1+bt-e^{-(\varepsilon-\lambda)t}}\right] \quad \text{(A4d)}$$

Although the ratio ^{40}Ar/^{40}K in Equation (A4d) is not strictly constant because it depends on the depositional age t, it may be nearly constant for some lengths of depositional age, varying by about ±2% of a constant apparent age, depending on the values of the K addition rate b and Ar release rate ε, both of an order of magnitude of about 1%/Ma or slightly higher.

As t approaches 0, the time-dependent terms in the numerator and denominator of the ratio within the square brackets, approach 0/0. By L'Hôpital's theorem, differentiation of the numerator and denominator with respect to t, gives the limit as $(\varepsilon - \lambda)/(b + \varepsilon - \lambda)$. Substitution of the latter in Equation (A4d) gives the ^{40}Ar/^{40}K ratio close to the initial value at time $t \to 0$:

$$\frac{^{40}\mathrm{Ar}}{^{40}\mathrm{K}} = \frac{\lambda_a}{\varepsilon-\lambda}\left[1 - \frac{b}{b+\varepsilon-\lambda}\right] \quad \text{(A4e)}$$

In the fitting of the measured K-Ar apparent ages that are approximately constant with increasing depositional age, as shown in Figures 5, 7 and 8. Equation (A4b) was used.

(b) Addition of K at an exponential rate (b) and ^{40}Ar release (first-order rate parameter ε)
The mass-balance equation is analogous to Equation (A4a):

$$d(^{40}\mathrm{Ar})/dt = \underset{\text{K addition,}}{\lambda_a {}^{40}\mathrm{K}_0 e^{(b-\lambda)t}} - \underset{^{40}\text{Ar growth}}{\varepsilon(^{40}\mathrm{Ar})} \quad \underset{^{40}\text{Ar escape}}{} \tag{A4f}$$

The solution is:

$$\frac{^{40}\mathrm{Ar}}{^{40}\mathrm{K}} = \frac{\lambda_a}{\varepsilon + b - \lambda}\left[1 - e^{-(\varepsilon+b-\lambda)t}\right] + \left(\frac{^{40}\mathrm{Ar}}{^{40}\mathrm{K}}\right)_0 e^{-(\varepsilon+b-\lambda)t} \tag{A4g}$$

5. Increase or decrease in the ^{40}Ar/^{40}K ratio and K-Ar apparent age with time

Changes in the ^{40}Ar/^{40}K ratio and the K-Ar apparent age, related to the ratio by Equation (A1d), are shown in Figure 3 for a closed system and examples of an open system with different rates of K addition, Ar release, and a combination of these two processes. Whether the ^{40}Ar/^{40}K ratio increases or decreases with time, that is represented by depositional time t or depth in the sediment on the vertical axis, depends on the values of the individual parameters, and the direction of change in the ^{40}Ar/^{40}K ratio is given by the derivative of the ratio with respect to time. The derivative

$$\frac{d(^{40}\mathrm{Ar}/^{40}\mathrm{K})}{\mathrm{dt}} \tag{A5a}$$

is positive if the ratio and K-Ar apparent age increase with time or it is negative when they decrease. For some relatively higher values of the linear rate of K addition (Figure 3, b = 0.05 Ma^{-1}), the ratio and the K-Ar apparent age may change their direction with increasing time. It should be pointed out that in a system containing no radiogenic ^{40}Ar initially, the ^{40}Ar/^{40}K ratio would increase from time t = 0. However, in an open system, if there is radiogenic ^{40}Ar present initially in the mineral particles, the apparent age may either increase or decrease.

5.1 For a closed system, differentiation of Equation (A1c) gives:

$$\frac{d(^{40}\mathrm{Ar}/^{40}\mathrm{K})}{\mathrm{dt}} = \left[\lambda_a + \lambda(^{40}\mathrm{Ar}/^{40}\mathrm{K})_0\right] e^{\lambda t} \tag{A5b}$$

In the preceding, the derivative is always positive and the ^{40}Ar/^{40}K ratio and K-Ar apparent age increase with time irrespective of the initial value of the (^{40}Ar/^{40}K)$_0$ ratio.

5.2 For an open system with ^{40}Ar release at a first-order rate ε and no K addition, differentiation of Equation (A2c) gives:

$$\frac{d(^{40}\mathrm{Ar}/^{40}\mathrm{K})}{\mathrm{dt}} = \left[\lambda_a - (\varepsilon - \lambda)(^{40}\mathrm{Ar}/^{40}\mathrm{K})_0\right] e^{-(\varepsilon-\lambda)t} \tag{A5c}$$

In the preceding, the derivative may be either positive or negative, depending on the values of the terms in square brackets, and the K-Ar apparent age may either increase or decrease with increasing time t or depth in the sediment.

5.3 For an open system with K addition at a linear rate b and no ^{40}Ar release, differentiation of Equation (A3c) gives:

$$\frac{d(^{40}\mathrm{Ar}/^{40}\mathrm{K})}{\mathrm{dt}} = \left[\frac{\lambda_a}{\lambda}\left(1 + \frac{b}{\lambda}\right) + \left(\frac{^{40}\mathrm{Ar}}{^{40}\mathrm{K}}\right)_0\right] \cdot \left(\lambda - \frac{b}{1+bt}\right) \cdot \frac{e^{\lambda t}}{1+bt} + \frac{\lambda_a b^2}{\lambda^2(1+bt)^2} \tag{A5d}$$

The derivative in Equation (A5d) may either be positive as shown in Figure 3 for the curves with b = 0.01 (curve 3a) where the apparent age increases, or the slope may change its sign from negative to positive, as in the case of b = 0.05 (curve 3b) where the apparent age initially decreases and later increases.

5.4 For an open system with K addition at an exponential rate b and ^{40}Ar release at a rate ε, it is algebraically simpler to consider the case of K_0e^{bt} than the linear case of addition, $K_0(1 + bt)$. Then, by differentiation of Equation (g), we obtain the derivative with respect to time:

$$\frac{d(^{40}\mathrm{Ar}/^{40}\mathrm{K})}{\mathrm{dt}} = \left[\lambda_a - (\varepsilon + b - \lambda)(^{40}\mathrm{Ar}/^{40}\mathrm{K})_0\right] e^{-(\varepsilon+b-\lambda)t} \quad \text{(A5e)}$$

The algebraic sign of the derivative depends on the magnitudes of the terms in square brackets and the ^{40}Ar/^{40}K ratio and the K-Ar apparent age may either increase or decrease with time, depending on the initial conditions and the rate parameter value.

References

1. Velde, B. (Ed.) *Origin and Mineralogy of Clays*; Springer: Berlin/Heidelberg, Germany, 1995; p. 334.
2. Kübler, B. Concomitant alteration of clay minerals and organic matter during burial diagenesis. In *Soils and Sediments—Mineralogy and Geochemistry*; Paquet, H., Clauer, N., Eds.; Spinger: Berlin/Heidelberg, Germany, 1997; pp. 327–362.
3. Kübler, B.; Goy-Eggenberger, D. La cristallinité de l'illite revisitée: Un bilan des connaissances acquises ces trente dernières années. *Clay Miner.* **2001**, *36*, 143–157. [CrossRef]
4. Clauer, N.; Chaudhuri, S. *Clays in Crustal Environments. Isotope Dating and Tracing*; Springer: Berlin, Germany, 1995; 359p.
5. Szczerba, M.; Derkowski, A.; Kalinichev, A.G.; Środoń, J. Molecular modeling of the effects of ^{40}Ar recoil in illite particles on their K–Ar isotope dating. *Geochim. Cosmochim. Acta* **2015**, *159*, 162–176. [CrossRef]
6. Clauer, N.; Środoń, J.; Francu, J.; Sucha, V. K-Ar dating of illite fundamental particles separated from illite/smectite. *Clay Miner.* **1997**, *32*, 181–196. [CrossRef]
7. Clauer, N.; Keppens, E.; Uysal, I.T.; Aubert, A. Ultrasonic shaking with diverse reagents of glauconite pellets for a comparison of their K-Ar with already published Rb-Sr results. *Geosciences* **2021**, *11*, 439. [CrossRef]
8. Clauer, N.; Cocker, J.D.; Chaudhuri, S. Isotopic dating of diagenetic illites in reservoir sandstones: Influence of the investigator effect. In *Origin, Diagenesis and Petrophysics of Clay Minerals in Sandstones*; SEPM Society for Sedimentary Geology: Broken Arrow, OK, USA, 1992; Volume 47, pp. 5–12.
9. Clauer, N. How Can Technical Aspects Help Improving K-Ar Isotopic Data of Illite-Rich Clay Materials into Meaningful Ages? The Case of the Dominique Peter Uranium Deposit (Saskatchewan, Canada). *Geosciences* **2020**, *10*, 285. [CrossRef]
10. Elliott, W.C.; Aronson, J.L.; Matisoff, G.; Gautier, D.L. Kinetics of the smectite to illite transformation in the Denver Basin; Clay mineral, K-Ar data and mathematical model results: American Association of Petroleum. *Geol. Bull.* **1991**, *75*, 436–462.
11. Mossmann, J.R. K-Ar dating of authigenic illite-smectite clay material: Application to complex mixtures of mixed-layer assemblages. *Clay Miner.* **1991**, *26*, 189–198. [CrossRef]
12. Velde, B.; Vasseur, G. Estimation of the diagenetic smectite to illite transformation in time-temperature space. *Am. Mineral.* **1992**, *77*, 967–976.
13. Huang, W.L.; Longo, J.M.; Pevear, D.R. An experimentally derived kinetic model for smectite-to-illite conversion and its use as a geothermometer. *Clays Clay Miner.* **1993**, *41*, 162–177. [CrossRef]
14. Elliott, W.C.; Matisoff, G. Evaluation of kinetic models for the smectite to illite transformation. *Clays Clay Miner.* **1996**, *44*, 77–87. [CrossRef]
15. Środoń, J. Extracting K-Ar ages from shales: A theoretical test. *Clay Miner.* **1999**, *33*, 375–378. [CrossRef]
16. Lerman, A.; Ray, B.M.; Clauer, N. Radioactive production and diffusional loss of radiogenic 40Ar in clays in relation to its flux to the atmosphere. *Chem. Geol.* **2007**, *243*, 205–224. [CrossRef]
17. Szczerba, M.; Środoń, J. Extraction of diagenetic and detrital ages and of the $^{40}K_{detrital}/^{40}K_{diagenetic}$ ratio from K-Ar dates of clay fractions. *Clays Clay Miner.* **2009**, *57*, 93–103. [CrossRef]
18. Dunoyer de Segonzac, G. The transformation of clay minerals during diagenesis and low-grade metamorphism: A review. *Sedimentology* **1970**, *15*, 281–346. [CrossRef]
19. Weaver, C.E.; Wampler, J.M. K, Ar, illite burial. *Geol. Soc. Am. Bull.* **1970**, *81*, 3423–3430. [CrossRef]
20. Boles, J.R.; Franks, S.G. Clay diagenesis in Wilcox sandstones of southwest Texas: Implications of smectite diagenesis on sandstone cementation. *J. Sediment. Petrol.* **1979**, *49*, 55–70.
21. Altaner, S.P. Comparison of Rates of Smectite Illitization with Rates of K-Feldspar Dissolution. *Clays Clay Miner.* **1986**, *34*, 608–611. [CrossRef]
22. Glasmann, J.R.; Larter, S.; Briedis, N.A.; Lundegard, P.D. Shale diagenesis in the Bergen High Area, North Sea. *Clays Clay Miner.* **1989**, *37*, 97–112. [CrossRef]
23. Awwiller, D.N. Illite/smectite formation and potassium mass transfer during burial diagenesis of mudrocks: A study from the Texas Gulf Coast Paleocene-Eocene. *J. Sediment. Petrol.* **1993**, *63*, 501–512.
24. Furlan, S.; Clauer, N.; Chaudhuri, S.; Sommer, F. K transfer during burial diagenesis in the Mahakam Delta Basin (Kalimantan, Indonesia). *Clays Clay Miner.* **1996**, *44*, 157–169. [CrossRef]
25. Perry, E.A., Jr. Diagenesis and the K-Ar dating of shales and clay minerals. *Geol. Soc. Am. Bull.* **1974**, *85*, 827–830. [CrossRef]
26. Faure, G. *Principles of Isotope Geology*, 2nd ed.; Wiley: New York, NY, USA, 1986; p. 589.

27. Clauer, N.; Chaudhuri, S. Inter-basinal comparison of the diagenetic evolution of illite/smectite minerals in buried shales on the basis of K-Ar systematics. *Clays Clay Miner.* **1996**, *44*, 818–824. [CrossRef]
28. Pollastro, R.M. Mineralogical and morphological evidence for the formation of illite at the expense of illite/smectite. *Clays Clay Miner.* **1985**, *33*, 265–274. [CrossRef]
29. Pollastro, R.M. Considerations and applications of the illite/smectite geothermometer in hydrocarbon-bearing rocks of Miocene to Mississippian age. *Clays Clay Miner.* **1993**, *41*, 119–133. [CrossRef]
30. Jennings, S.; Thompson, G.R. Diagenesis of Plio-Pleistocene sediments of the Colorado River delta, southern California. *J. Sediment. Petrol.* **1986**, *56*, 89–98.
31. Freed, R.L.; Peacor, D.R. Diagenesis and the formation of authigenic illite-rich crystals in Gulf Coast shales: TEM study of clay separates. *J. Sediment. Petrol.* **1992**, *62*, 220–234.
32. Milliken, K.L. Chemical behavior of detrital feldspars in mudrocks versus sandstones, Frio Formation (Oligocene), South Texas. *J. Sediment. Petrol.* **1992**, *62*, 790–801.
33. Kübler, B. La cristallinité de l'illite et les zones tout à fait supérieures du métamorphisme. In *Colloque sur les Etages Tectoniques*; La Baconnière: Neuchatel, Switzerland, 1966; pp. 105–122.
34. Hower, J.; Eslinger, E.V.; Hower, M.; Perry, E.A. Mechanism of burial metamorphism of argillaceous sediments: 1. Mineralogical and chemical evidence. *Geol. Soc. Am. Bull.* **1976**, *87*, 725–737. [CrossRef]
35. Clauer, N.; Rinckenbach, T.; Weber, F.; Sommer, F.; Chaudhuri, S.; O'Neil, J.R. Diagenetic evolution of clay minerals in oil-bearing Neogene sandstones and associated shales, Mahakam Delta Basin, Kalimantan, Indonesia. *Am. Assoc. Pet. Geol. Bull.* **1999**, *83*, 62–87.
36. Aronson, J.L.; Hower, J. Mechanism of burial metamorphism of argillaceous sediments: 2. Radiogenic argon evidence. *Geol. Soc. Am. Bull.* **1976**, *87*, 738–744. [CrossRef]
37. Eberl, D.D. Three zones for illite formation during burial diagenesis and metamorphism. *Clays Clay Miner.* **1993**, *41*, 26–37. [CrossRef]
38. Lerman, A.; Clauer, N. Loss of radiogenic ^{40}Ar in the fine-clay size fractions of sediments. *Clays Clay Miner.* **2005**, *53*, 234–249. [CrossRef]
39. 3D Paleogeographic and Plate Tectonic Reconstructions: The PALEOMAP Project is Back in Town. *Houst. Geol. Soc. Bull.* **2002**, *44*, 13–15.
40. Clauer, N.; Chaudhuri, S. Extracting K-Ar ages from shales: The analytical evidence. *Clay Miner.* **2001**, *36*, 227–235. [CrossRef]
41. Steiger, R.H.; Jäger, E. Subcommission on Geochronology: Convention on the use of decay constants in Geo- and Cosmochronology. *Earth Planet. Sci. Lett.* **1977**, *36*, 359–362. [CrossRef]
42. Clauer, N.; Rousset, D.; Środoń, J. Modeled shale and sandstone burial diagenesis based on the K-Ar systematics of illite-type fundamental particles. *Clays Clay Miner.* **2004**, *52*, 576–588. [CrossRef]
43. Odin, G.S.; Hunziker, J.C. Étude isotopique de l'altération naturelle d'une formation a glauconie (méthode à l'argon). *Contrib. Mineral. Petrol.* **1974**, *48*, 9–22. [CrossRef]
44. Hunziker, J.C.; Frey, M.; Clauer, N.; Dallmeyer, R.D.; Friedrichsen, H.; Flehmig, W.; Hochstrasser, K.; Roggwiler, P.; Schwander, H. The evolution of illite to muscovite: Mineralogical and isotopic data from the Glarus Alps, Switzerland. *Contrib. Mineral. Petrol.* **1986**, *92*, 157–180. [CrossRef]
45. Hassanipak, A.A.; Wampler, J.M. Radiogenic argon released by stepwise heating of glauconite and illite: The influence of composition and particle size. *Clays Clay Miner.* **1996**, *44*, 717–726. [CrossRef]
46. Lee, J.-Y.; Marti, K.; Severinghaus, J.P.; Kawamura, K.; Yoo, H.-S.; Lee, J.B.; Kim, J.S. A redetermination of the isotopic abundances of atmospheric Ar. *Geochim. Et Cosmochim. Acta* **2006**, *70*, 4507–4512. [CrossRef]
47. Środoń, J.; Clauer, N.; Eberl, D.D. Interpretation of K-Ar dates of illitic clays from sedimentary rocks aided by modeling. *Am. Mineral.* **2002**, *87*, 1528–1535. [CrossRef]
48. McCarty, D.K.; Sakharov, B.A.; Drits, V. Early clay diagenesis in Gulf Coast sediments: New insights from XRD profile modeling. *Clays Clay Miner.* **2008**, *56*, 359–379. [CrossRef]
49. Odin, G.S. *Green Marine Clays. Developments in Sedimentology, 45*; Elsevier Science Publishers: Amsterdam, The Netherlands, 1988.